UNITED AIRCRAFT CORPORATION

United Aircraft Research Laboratories

EAST HARTFORD, CONNECTICUT

United Aircraft Research Laboratories

UNITED AIRCRAFT CORPORATION

EAST HARTFORD, CONNECTICUT 06108

Report K-910900-9

Initial Experiments to Investigate Condensation of Flowing Metal-Vapor/ Heated-Gas Mixtures in a Duct

Contract No. SNPC-70

REPORTED BY Harold E Bauer
Harold E. Bauer

APPROVED BY James W. Clark
James W. Clark, Chief
Fluid and Systems Dynamics

DATE September 1971

NO. OF PAGES 44

COPY NO. 26

FOREWORD

An exploratory experimental and theoretical investigation of gaseous nuclear rocket technology is being conducted by the United Aircraft Research Laboratories under Contract SNPC-70 with the joint AEC-NASA Space Nuclear Systems Office. The Technical Supervisor of the Contract for NASA was Captain C. E. Franklin (USAF) for the first portion of the contract performance period and was Dr. Karlheinz Thom for the last portion of the contract performance period. Results obtained during the period September 16, 1970 and September 15, 1971 are described in the following seven reports (including the present report) which comprise the required second Interim Summary Technical Report under the Contract:

1. Roman, W. C. and J. F. Jaminet: Experimental Investigations to Simulate the Thermal Environment and Fuel Region in Nuclear Light Bulb Reactors Using an R-F Radiant Energy Source. United Aircraft Research Laboratories Report K-910900-7, September 1971.

2. Klein, J. F.: Experiments to Simulate Heating of the Propellant in a Nuclear Light Bulb Engine Using Thermal Radiation from a D-C Arc Radiant Energy Source. United Aircraft Research Laboratories Report K-910900-8, September 1971.

3. Bauer, H. E.: Initial Experiments to Investigate Condensation of Flowing Metal-Vapor/Heated-Gas Mixtures in a Duct. United Aircraft Research Laboratories Report K-910900-9, September 1971. (present report)

4. Rodgers, R. J., T. S. Latham and H. E. Bauer: Analytical Studies of Nuclear Light Bulb Engine Radiant Heat Transfer and Performance Characteristics. United Aircraft Research Laboratories Report K-910900-10, September 1971.

5. Latham, T. S. and H. E. Bauer: Analytical Design Studies of In-Reactor Tests of a Nuclear Light Bulb Unit Cell. United Aircraft Research Laboratories Report K-910900-11, September 1971.

6. Krascella, N. L.: Spectral Absorption Coefficients of Helium and Neon Buffer Gases and Nitric Oxide-Oxygen Seed Gas Mixture. United Aircraft Research Laboratories Report K-910904-2, September 1971.

7. Palma, G. E. and R. M. Gagosz: Effect of 1.5 Mev Electron Irradiation on the Transmission of Optical Materials. United Aircraft Research Laboratories Report K-990929-2, September 1971.

Report K-910900-9

Initial Experiments to Investigate Condensation of Flowing Metal-Vapor/Heated-Gas Mixtures in a Duct

TABLE OF CONTENTS

Report K-910900-9

Initial Experiments to Investigate Condensation of Flowing Metal-Vapor/Heated-Gas Mixtures in a Duct

SUMMARY

An exploratory experimental study of the condensation of a metal vapor carried in a flowing stream of non-condensible gas in a duct was conducted to provide information which could be used in the design of the cavity exhaust ports of a nuclear light bulb engine and an in-reactor test unit. Condensation was initiated by adding a sufficient quantity of cold non-condensible gas to a heated vapor/gas mixture to reduce the mixed mean temperature to a level below the melting point of the condensible material. It is desired to have condensation occur in the flowing gas with minimum deposition of condensible material on the duct walls.

A series of preliminary tests were conducted using iodine and air as the vapor/gas mixture. The air and iodine were heated electrically in an oven to produce the heated vapor/gas mixture which was then cooled by mixing with additional cold air at the inlet to a 1.0-m (39.4-in.)-long pyrex tube test section. Subsequent test series were conducted using zinc and argon as the vapor/gas mixture. Argon was preheated using a d-c arc plasma torch and was then passed through a vaporizer section containing zinc. At the test section, cold argon was used to cool the mixture. Two inlet configurations for the cold gas were used, one with direct radial inflow (no swirl) and one with rotating inflow (swirl). In addition, tests were conducted with heated and unheated test section walls.

In the iodine/air tests, condensation on the test section walls could be eliminated by maintaining the test section walls at a temperature approximately 10 to 15 K above the mixed-mean temperature of the flow in the tube. In the zinc/argon tests, heating of the tube walls had no observable effect on the amount of deposition on the tube walls. This difference is believed to be due to the different amounts of mixture sub-cooling present in the tests. A weight flow of cold argon gas equal to at least 10 times the weight flow of vapor/gas mixture was required to rapidly condense the zinc vapor into particulate form away from the test section walls.

The results of these exploratory tests indicate the need for additional experiments in which measurements of particle size, amount of wall coating, velocity distributions, and temperature distributions within the duct and at the duct wall are made. These experiments should concentrate on the zinc/argon system or other metal-vapor/gas systems, rather than on the iodine/air system because the operating conditions of such tests would more closely simulate the heat transfer and condensation processes in nuclear light bulb reactor exhaust ducts.

RESULTS AND CONCLUSIONS

1. It is possible to condense a metal vapor in a flowing stream without condensation on the duct walls if a sufficient quantity of cold gas is added to the vapor/gas mixture at the test section inlet. Tests with zinc as a condensible material indicate that the required ratio of cold gas to heated vapor/gas mixture is approximately 10 to 1. At this flow ratio, or above, any wall coating which occurs can be wiped off after the test. At lower flow ratios, a plating is noted which cannot be wiped off, probably caused by vapor or liquid contacting the walls. The amount of plating generally increases as the flow ratio is reduced.

2. The total quantity of zinc particles which adhered to the test section walls during a series of runs was between 5 and 10 percent of the total weight of zinc which passed through the tube.

3. The size of the particles formed during condensation appears to be dependent on the physical properties of the condensible material and on the ratio of cold gas to heated-vapor/gas mixture. The characteristic sizes of the iodine particles formed were on the order of 500 microns while the zinc particles were on the order of 0.05 to 1 micron. The 1-micron zinc particles were formed at flow ratios of approximately 6 to 1 and the 0.05 micron particles were formed at flow ratios of 11 to 1.

4. In the iodine/air tests, condensation on the test section walls could be eliminated by maintaining the test section walls at a temperature approximately 10 to 15 K above the mixed-mean temperature of the iodine/air mixture in the tube. In the zinc/argon experiments, heating of the tube walls had no observable effect on the amount of particulate deposition or plating on the walls. This difference is believed due to the fact that the addition of cold bypass gas brought the mixed-mean temperature only slightly below saturation in the iodine/air tests, while the mixed-mean conditions were substantially sub-cooled in the zinc/argon tests.

INTRODUCTION

Investigations of various phases of gaseous nuclear rocket technology are being conducted at the United Aircraft Research Laboratories under Contract SNPC-70 administered by the joint AEC-NASA Space Nuclear Systems Office. Previous investigations were conducted under NASA Contracts NASw-847, NASw-768, and NAS3-3382; under Air Force Contracts AF 04(611)-7448 and AF 04(611)-8189; and under Corporate sponsorship.

The principal research effort is presently directed toward the closed-cycle, vortex-stabilized nuclear light bulb engine. This engine concept is based on the transfer of energy by thermal radiation from gaseous fissioning uranium, through a transparent wall, to hydrogen propellant. The engine is comprised of seven unit cavities, each having its own fuel, transparent wall and propellant duct. The basic design of the engine is described in detail in Ref. 1. Subsequent investigations, which were performed to supplement and investigate the basic design and to investigate other phases of nuclear light bulb engine component development, are reported in Refs. 2 through 5. Reference 6 includes a summary of pertinent nuclear light bulb research conducted through November 1969.

A mixture of buffer gas, fuel and fission fragments is exhausted from each unit cavity through a port located at the center of one or both end walls. The average temperature of the gases entering the exhaust duct is expected to be about 6550 K (11,800 R) in the reference engine cavity. In a test of a small unit cavity which could be installed in the LASL Nuclear Furnace reactor, the average temperature would be about 4800 K (8640 R). Continuous operation of the engine is dependent upon the ability to condense and separate the entrained fuel from these gases so that both the fuel and the buffer gas may be recycled separately. This condensation and separation at the thru-flow exhaust ducts, therefore, is an important consideration in demonstrating the feasibility of the closed-cycle concept. In addition, it is necessary to develop the condensation technology (although not necessarily the separation technology) before in-reactor tests can be undertaken.

The primary objective of the research reported herein was to provide needed information from which the flow conditions and injection methods required to rapidly cool the vapor/gas mixture in the exhaust duct of a reference engine or in-reactor test unit cell may be determined. This work involved performing limited theoretical investigations and exploratory tests from which qualitative information was obtained on the condensation of a metal-vapor/gas mixture in a flowing stream, while minimizing the deposition of condensed material on the surrounding duct walls.

DISCUSSION OF TEST OBJECTIVES AND SIMULATION REQUIREMENTS

In the reference engine, the exhaust flow is a high-temperature mixture of vaporized uranium and neon gas; in the in-reactor test unit, the exhaust is a uranium/argon mixture. Both the engine and the in-reactor test would operate at a pressure level of 500 atm. For these initial condensation tests, it was proposed that condensation phenomena be investigated at relatively low temperatures. Before the test apparatus could be designed, it was necessary to conduct some preliminary investigations, including (1) consideration of the proposed configuration and operating conditions in both the reference engine and in-reactor test unit to determine the fixed and variable parameters, (2) comparison of the physical properties of various low-melting-point materials (particularly vapor pressures) to determine the operating requirements of the test apparatus, and (3) investigation of the similarity parameters for scaling between test results and actual engine or in-reactor test unit conditions.

Simulation Requirements for Reference Engine and In-Reactor Test Unit Cell

The unit cavity of the reference engine consists of a fissioning uranium plasma contained in a vortex which is driven by the tangential injection of neon gas at the inside of a circular transparent wall. The neon which drives the vortex, together with some fission products and entrained uranium vapor, exits the cavity through an exhaust port in one or both end walls. This exhaust flow will have a rotational component, or swirl, as it exits. The overall coolant circuitry for the reference engine is shown in Fig. 1. To operate the engine continuously for long periods of time, it is necessary to recover the uranium which is entrained in the neon and to recycle the uranium and neon in separate circuits. As shown in the fuel and neon circuit at the bottom of Fig. 1, the proposed method of operation is to cool the exhaust by the addition of cold neon which has bypassed the cavity. The uranium/neon mixture is cooled sufficiently to condense the uranium to solid form so that it can be separated from the neon. The neon is then cooled by rejecting heat to the primary propellant flow in the hydrogen-neon heat exchanger shown in Fig. 1. The cold neon must be introduced in a manner such that the exhaust flow is quickly cooled to protect the exhaust tube from the high-temperature exhaust flow. Moreover, condensation must occur in the stream, rather than on the exhaust tube walls.

The in-reactor test unit cell is similar in its basic principle of operation but uses argon gas to drive the vortex. At present, there are no plans to separate or recycle the fuel and argon during operation of the in-reactor tests; the small size of the unit cell will permit reasonable run times with relatively low total fuel and argon requirements. It is, however, still necessary to cool the exhaust mixture enough to protect the exhaust tube walls from hot gases, and to minimize condensation of fissionable fuel on the walls.

Proposed Configurations

Proposed geometries of the cavity and exhaust ports for the in-reactor test unit cell with centerline fuel injection and with off-center fuel injection are shown in Figs. 2 and 3, respectively. If centerline fuel injection is employed, the exhaust port is annular and cold gas must be injected from both sides of the annulus (Fig. 2). If the fuel is injected off-center, the exhaust port is cylindrical, and the geometry is simplified as shown in Fig. 3. It may be desirable to bring the cold gas up to the cavity end wall region in one or more tubes, separate from the exhaust duct, rather than in the annular configuration shown in Figs. 2 and 3, to minimize heat transfer between the exhaust flow and the cold gas. It should be mentioned that details shown in the left-hand portions of Figs. 2 and 3 are still uncertain; the allowable lengths of the exhaust tubes, for example, will depend on how well the fuel can be kept off the walls.

The reference engine unit cavity would have a configuration similar to the in-reactor test unit cell with regard to the cavity interior, exhaust flow port and cold gas injectors. The choice of centerline or off-center fuel injection for the reference engine is still open. The cavity inside diameter is 48.9 cm (19.35 in.) and its length is 1.83 m (6 ft). The dimensions of the exhaust ports were considered to be a design variable since in previous designs of both the in-reactor test unit and the reference engine (see Refs. 2 and 3) the duct size was based on the size required to give a reasonable pressure loss in the duct ($\cong$ 4 atm) when sufficient cold gas had been added to reduce the temperature of the cavity exhaust and cold gas to 1390 K (2500 R).

Operating Conditions

In the in-reactor test unit cell, 25.3 gm/sec (5.6×10^{-2} lb/sec) of argon at a temperature of 555 K (1000 R) is injected to drive the vortex. In passing through the cavity it entrains 1.59 gm/sec (3.5×10^{-3} lb/sec) of fuel, and is heated by conduction and convection from the fuel region. In the reference engine, the neon flow in each of the seven cavities is 1590 gm/sec (3.5 lb/sec) at an injection temperature of 1110 K (2000 R). The calculated inlet conditions at the exhaust flow ports for both the engine and the in-reactor unit are given in Table I. The operating pressure level for both units is 500 atm, which results in a calculated uranium partial pressure of 5.2 atm in the in-reactor test unit exhaust and 12 atm in the reference engine exhaust. The calculated bypass flow rate shown in Table I is based on the quantity of cold gas required to reduce the mixed-mean temperature of the mixture of exhaust flow and bypass to 1390 K (2500 R).

Properties of Low-Boiling-Point Metals

In analyzing the metals which might be used to simulate uranium in the experimental program, primary consideration was given to metals with reasonably high vapor pressures in the temperature range of 500 to 1500 K (900 to 2700 R). These temperature levels are attainable using a small d-c arc plasma torch. Also, conventional

materials could be used in the test apparatus. The alkali metals (sodium, potassium, lithium and cesium) were eliminated due to their handling difficulties, and mercury was eliminated due to its extremely low freezing point. The melting points and vapor pressures of those metals considered are shown in Fig. 4. Of the materials shown, iodine and zinc were selected for this initial test series. Other materials which could be employed without modification of the present test apparatus are cadmium, bismuth and antimony. The higher temperature levels which would be necessary for producing the required partial pressures with tin or lead as a metal vapor would require an externally cooled wall in the vaporizer section.

Similarity Parameters Investigated

To determine the desired operating conditions for the test apparatus and to relate the results of the tests to the reference engine and in-reactor test unit, it was necessary to investigate the conditions which were to be simulated and to make some preliminary assumptions as to the major parameters which would affect the condensation processes. The parameters considered were (1) the vapor/gas mass flow rate ratio, (2) the vapor partial pressure, (3) the superheating or subcooling of the vapor in the exhaust flow, and (4) the flow and geometric parameters.

Vapor/Gas Mass Flow Rate Ratio

Since the mass flow rate of fuel, fuel carrier gas and buffer gas is known for both the reference engine and the in-reactor test unit, the vapor/gas mass flow rate ratio in the exhaust flow can be calculated. In a mixture of gases in equilibrium, the relation between the partial pressures and the mass of gas present may be expressed as

$$\frac{P_x}{P_y} = \frac{M_x}{M_y}\,\frac{m_y}{m_x} \qquad (1)$$

where P is the partial pressure, M is the mass, m is the molecular weight and the subscripts, x and y, refer to the constituents of a two-gas mixture.

If the exhaust flow is considered to be an equilibrium mixture of metal vapor and gas which remains constant with time, the mass ratio may be replaced by the mass flow rate ratio, so that

$$\frac{P_v}{P_g} = \frac{w_v}{w_g}\,\frac{m_g}{m_v} \qquad (2)$$

where w is the mass flow rate and the subscripts v and g refer to the vapor and gas, respectively. Equation (2) relates the mass flow rate ratio (listed in Table I) to the partial pressure ratio. Hence, the mass flow rate ratio was used as the primary flow parameter in the experiments.

Partial Pressure of Vapor

The partial pressure of the vapor in the exhaust flow is calculated from Eq. (2) and the known operating pressure of the system by assuming an equilibrium, two-component gas mixture; hence, $P_v = P_t - P_g$, where P_t is the total pressure or operating pressure level. The uranium partial pressure and temperature conditions in the exhaust of the reference engine and the in-reactor test unit cell are shown in Fig. 5. In the reference engine, the vapor in the exhaust flow is superheated; in the in-reactor test unit the vapor is at saturation conditions or slightly above, depending upon the exact operating conditions selected.

If the mass flow rate ratio is taken as the fixed parameter, then the partial pressure ratio will be affected by the molecular weight ratio of the vapor/gas mixture used in the experiment. The molecular weight ratio, m_g/m_v, for the reference engine (neon/uranium) is 0.0851, and the molecular weight ratio for the in-reactor test unit (argon/uranium) is 0.1702. For the two test series in the present investigation, the molecular weight ratios for an iodine/air mixture and a zinc/argon mixture are 0.11 and 0.61, respectively. Therefore, if the mass flow rate ratio is matched, the partial pressure ratio in a zinc/argon system, for example, will be approximately eight times as high as in a uranium/neon system. The partial pressures and corresponding temperatures required to match the mass flow rate ratios, w_v/w_g, of the reference engine, for all of the low-melting-point materials considered, are shown on Fig. 4. Argon and helium were considered as possible inert gases to determine if the lower molecular weight of helium would appreciably lower the required operating temperatures. Air was not considered for use with metal vapors because of the possibility of chemical reaction with the metal.

Superheat of Vapor

As previously mentioned, the vapor in the exhaust of the reference engine and in-reactor test will be superheated to some degree. To calculate the amount of superheat required in the experimental apparatus, a proportionality between the degree of superheat and the difference between the melting point of the metal and the saturation temperature at the required partial pressure was assumed. For example, in the reference engine (see Fig. 5) the uranium partial pressure is 12 atm, the exhaust temperature is 6550 K (11,800 R), the melting point is 1406 K (2540 R) and the saturation temperature at 12 atm partial pressure is 5220 K (9400 R). The ratio of superheat to the difference between melting and saturation is 0.349. For an experiment using zinc and argon, the required zinc partial pressure is 0.156 atm, so that the saturation temperature is 1075 K (1990 R) and the melting point is 692 K (1245 R). The required superheat for the zinc system would be approximately 134 K (241 R).

Flow and Geometric Parameters

Estimated mass flow rates and mixed-mean temperatures at the entrance to the exhaust duct are given in Table I for reference engine and in-reactor test conditions. At present, needed additional information on the temperature distribution, concentration distribution of the condensible vapor, and velocity distribution at the duct entrance is not available. The exhaust duct dimensions were calculated by assuming a value of the ratio of bypass gas to heated vapor/gas mixture and sizing the duct to have a pressure loss of approximately 4 atm at the required mass flow rate.

The test section geometry and inlet configuration used in the tests was designed to provide a capability for use of several flow injection methods. The test section dimensions and flow rates used were such that turbulent flow should have existed in the test section.

Because an exact model of the reference engine or in-reactor test exhaust geometry was not employed, it is necessary to identify, if possible, pertinent flow, heat transfer, and geometric similarity parameters so that the test results can be scaled to reference engine and in-reactor test conditions. Existing information on evaporation and condensation phenomena is primarily applicable to systems in which condensation occurs at a uniform rate throughout the mixture and not systems subjected to rapid changes in temperature or vapor concentration. The requirement that the condensation, to a solid form, be achieved in a short time and that vapor or liquid be kept away from the wall can only be met by establishing a steep temperature and concentration gradient in the inlet region. It may be possible to calculate values for these parameters based on averaged conditions in the inlet region.

DISCUSSION OF TESTS

The preliminary experiments conducted using iodine/air mixtures and the subsequent tests conducted using zinc/argon mixtures represent two different regimes of operation. As shown by the upper shaded area in Fig. 4, the iodine/air tests were in an operating range where the mixed-mean temperature and partial pressure of the mixture after the addition of cold bypass air were very close to the saturation conditions. As a result, considerable amounts of vapor were present in the flow throughout the entire length of the exhaust duct. In the zinc/argon tests, the mixed-mean temperature and partial pressure were much further from the saturation conditions (see lower shaded area in Fig. 4). The two sets of experiments are discussed separately here. The zinc/argon tests best simulate the conditions desired in the reference engine and in-reactor test unit.

Iodine/Air Experiments

Test Apparatus

A sketch of the test apparatus used in the iodine/air experiments is shown in Fig. 6. The iodine/air mixture was produced by passing air through a preheater coil and a series of three iodine boilers contained in a constant-temperature oven (not shown). The flow rate of air through the coil and boilers was sufficiently low so that the air became saturated with iodine vapor at the oven temperature. The mixture was then passed through a heated tube to the inlet where it entered the test section without swirl, as shown on Fig. 6. At the entrance to the 2.5-cm (1.0-in.)-ID pyrex tube test section, cold bypass air was added, and all of the flow then passed through the test section.

At the downstream end, a cold trap was used to condense iodine vapor which remained in the stream before exhausting the air (Fig. 6). The cold trap consisted of a coil immersed in ethylene glycol which was cooled prior to a test run by the addition of dry ice. The air exiting the cold trap was bubbled through a sodium hypochlorite solution to absorb any iodine which might be carried through the cold trap.

During the experiments with heated tube walls, the test section was heated by resistance heater tapes wrapped around the outside of the pyrex tube. The power to these tapes was controlled by rheostats so that the wall temperature could be varied.

Three bypass configurations were investigated: (1) a straight nozzle as shown in Fig. 6 in which the bypass air was added coaxially with the iodine/air mixture; (2) a radial-inflow geometry, similar to that shown in Fig. 6 with the nozzle removed, in which the bypass air met the iodine/air mixture at right angles to promote mixing; and (3) a swirling inflow configuration in which the swirling bypass air was added to the non-swirling iodine/air mixture as shown in Fig. 7.

Test and Data Reduction Procedures

Prior to a test sequence, the ovens containing the air preheating coil and the iodine boilers were brought up to the temperature level required to produce the desired iodine partial pressure by thermostatically controlled resistance heaters. The valving in the ovens was arranged so that the iodine boilers could be bypassed. Once the desired initial test conditions were selected, all of the flows and resistance heater settings were made, and the test apparatus was run without iodine until it reached thermal equilibrium. After steady-state conditions were reached, the preheated air flow was routed through the iodine boilers so that an iodine/air mixture was introduced.

The normal test procedure was to establish an initial condition in which no condensation on the test section walls occurred. After operating at this condition, the ratio of cold air to heated iodine/air mixture was varied by changing the flow of cold air or the flow to the ovens. The flow ratio of cold gas to heated vapor/gas mixture was generally decreased until condensation occurred on the wall. The presence of condensation on the walls was determined by visual observation of the test section during operation.

During a test run, the air flow rates were monitored and temperature measurements were made at the iodine boiler, iodine/air inlet, cold air inlet and the test section outlet. The inlet air pressures, iodine boiler pressure and exit pressure from the test section were also monitored. The inlet region of the test section was periodically disassembled and inspected to determine if condensation was occurring in this region.

The data reduction procedure followed in analyzing the test data included (1) calculation of the mass flow rate of iodine based on the air mass flow rate, the total pressure and the temperature in the iodine boilers, (2) calculation of the mixed-mean temperature of the vapor/gas mixture after the addition of cold gas, and (3) calculation of the wall temperatures based on the temperature rise in the test section and standard flow and heat transfer calculations.

Results of Experiments

A conclusion of the iodine/air tests is that one way to prevent condensation on the test section wall is to maintain the wall temperature higher than the mixed-mean temperature of the vapor/gas mixture. However, subsequent experiments with zinc/argon mixtures indicated that some qualification of this conclusion is required. It appears that the use of heated walls to eliminate condensation is only applicable when the conditions in the test sections are close to saturation conditions. The disadvantage of operating in this regime is that a considerable amount of vapor still exists in the test section and, although the problem of wall deposition is eliminated, the vapor is not completely condensed and ready for separation at the end of the test section.

No detailed post-test inspection was performed after the iodine test runs since the relatively high vapor pressure of iodine at room temperature causes sublimation of the iodine particles when exposed. Estimates of the size of iodine

particles observed in the test section during two test runs were made from high-speed photographs of the test section during a run. Those particles which were observed were on the order of 500 microns in size.

Effects of Heating Tube Walls

The results of two test runs conducted using heated tube walls are shown in Fig. 8. The results indicate that a difference between the mixed-mean temperature of the iodine/air mixture and the temperature of the test section wall of 10 to 15 K (18 to 27 R) is sufficient to eliminate wall deposition. In all cases where wall deposition did occur it begins in liquid form and then solidifies if the wall temperature level is reduced. Additional data is listed in Table II.

Effects of Inlet Geometry

Of the three bypass inlet geometries investigated, the swirling inflow geometry was the most satisfactory for minimizing condensation in the inlet region. The nozzle configuration shown in Fig. 6 is unsatisfactory since it is cooled by the cold bypass air entering the inlet; iodine tends to condense on the inside of the nozzle. The inlet with the nozzle removed (radial inflow) did not have uniform flow around the entrance circumference and condensed iodine was found on one side of the test section after a series of tests. Apparently the heated iodine/air mixture was forced towards the wall by the non-uniform radial inflow. With this configuration it was also noted that condensation in the test section always started at the inlet end. With the swirling inflow geometry (see Fig. 7), when condensation occurred it was observed along the entire length of the tube. There was no condensed iodine in the inlet region after tests with swirling inflow.

Zinc/Argon Experiments

Test Apparatus

A sketch of the test apparatus used in the zinc/argon experiments is shown in Fig. 9. The zinc/argon mixture was produced by preheating the argon in a d-c arc plasma torch. The heated argon then passed through a 32-mm (1.26-in.)-ID Vycor tube containing metallic zinc. The heated gas melted the zinc during the start-up transient and then vaporized a portion of the zinc to form a zinc/argon mixture. This mixture then passed into the inlet region of the test section where cold argon bypass was added. The inlet and test section configuration were essentially similar to the iodine/air test apparatus. A photograph of the test apparatus is shown in Fig. 10.

A detailed cross-section of the d-c arc plasma torch is shown in Fig. 11. Argon was injected through a series of ports in the base of the anode. The injection ports were oriented to produce a swirling flow in a counterclockwise direction, viewed from the cathode end of the torch. The d-c arc discharge between the cathode tip and anode surface was rotated by applying a magnetic field. The arc rotation increased the transfer of energy to the argon and prevented the arc from attaching to a single point on the anode. The power supply used for the d-c

arc plasma torch was a Saban 50-kva d-c power supply powered by 460-480-v, 100-a, three-phase service. The maximum d-c current output of the power supply is 240 a at 216 v. In the flow and pressure regimes used in these tests, the voltage drop across the d-c arc plasma torch was on the order of 30 v, which allows an input power to the torch of 6 to 7 kw. The efficiency of the plasma torch, i.e., the ratio of power deposited in the argon flow to total input power, was approximately 20 percent for all tests in this series. The plasma torch configuration shown has been operated at total input power levels of up to 50 kw. This range of operating powers would permit operation at higher temperatures and higher argon mass flow rates without modifications to the torch in future tests.

It was determined during the preliminary tests that the zinc/argon mixture exiting the vaporizer was superheated, rather than saturated, probably due to the short residence time of the argon in the vaporizer. It was also determined that the mass flow rate of zinc could be increased by placing a larger amount of zinc in the vaporizer, thereby increasing the surface area of the molten zinc. If it is desired in future tests to increase the zinc mass flow rate to approach saturation conditions, the vaporizer section can be lengthened to increase the argon residence time.

The inlet region was designed so that the type of cold bypass gas injection could be changed by replacing a single part inside the inlet plenum. Two configurations were tested: (1) one with swirling flow, with the swirl in the same direction as the swirl in the torch (see Fig. 12), and (2) one with radial inflow, as shown in Fig. 13. The radial inflow configuration employed several layers of screen between the walls of the plenum region to insure a uniform flow distribution.

The test section was a 25-mm (1-in.)-ID pyrex tube similar to those used in the iodine/air tests. In tests with heated tube walls, the outside surface of the test section was heated by resistance heater tapes. After exiting the test section, the zinc/argon mixture was passed through a water scrubber system to remove any particulate zinc before exhausting the argon.

Test and Data Reduction Procedures

Tests with the zinc/argon apparatus differed from the iodine/air tests in that (1) it was not possible to reach thermal equilibrium before introducing the vapor so that a start-up transient occurs, (2) the requirement for higher wall temperatures required that the tube be completely wrapped with heater tapes so that the test section walls could not be observed during a test run, and (3) some form of wall deposition always occurred so that it was not possible to make a series of test runs to determine conditions leading to the onset of condensation.

The test procedure for the zinc/argon tests was to assemble the test apparatus with metallic zinc in the vaporizer, establish the desired argon flow rates in the torch and the cold-gas inlet, and then start the torch and bring it to the desired power level. It was determined that there was a minimum mass flow rate of argon through the torch required to insure starting. If the desired flow rate for the test was below this level, the flow was adjusted downward after starting.

After starting the plasma torch, thermal equilibrium was reached in all components after approximately 20 sec. The total run times for the tests ranged between 2 and 8 min. After each test, the test section was removed from the apparatus and various post-test inspection and sampling procedures were used.

The measurements made during a test run were similar to those in the iodine/air experiments. Argon flow rates, temperatures and pressures at the inlet to the torch and the cold gas inlet were measured. The temperature of the zinc/argon mixture exiting the vaporizer section was measured, as were the temperature and pressure of the mixture exiting the test section. In addition, the cooling water flow rates and temperature rises in the cathode, anode and magnet coils of the torch were measured to check the overall heat balance and determine the efficiency of the torch. The amounts of zinc in the vaporizer before and after a test were measured to obtain an approximation of the zinc mass flow rate during the test.

The data reduction procedures used were similar to those in the iodine/air tests except that the zinc mass flow rate was approximated directly from the zinc loss and run time, and zinc partial pressures were calculated on the basis of the zinc and argon mass flow rates. Mixed-mean temperatures and tube wall temperatures were calculated by the same procedures used in the iodine/air tests.

Since some type of deposition, either plating or particulate coatings, occurred in all of the zinc/argon tests, post-test inspection and sampling of the test section was of primary importance. Most of the test section tubes were wiped out after the test run to qualitatively determine if the coatings were removable particles or a coating which adhered to the wall. Samples were taken from five of the test sections prior to cleaning so that photomicrographs could be taken of the samples to determine particle size and form. Three of the test sections were cleaned by dissolving the coatings in hydrochloric acid to determine the total weight of zinc deposited on the wall during the test run.

Results of Experiments

The results of the zinc/argon experiments indicated that the vapor could be condensed in the flowing stream with little or no non-removable plating on the duct wall if the ratio of cold bypass gas to heated vapor/gas mixture was on the order of 10 to 1 or higher. At these flow ratios there was a particulate deposition on the walls which could be wiped off after a test. In the tubes which were subjected to chemical removal of the particulate deposit, the deposit was between 5 and 10 percent of the total mass of zinc which had passed through the tube during the test. The size of the particles formed also appeared to be dependent upon the flow ratio of cold bypass gas to heated vapor/gas mixture, with particle size decreasing as the flow ratio increased.

The partial pressure and temperature conditions in the zinc/argon mixtures before and after the addition of cold bypass gas are shown in Fig. 14. With the vaporizer configuration used, the zinc/argon mixture exiting the vaporizer was superheated rather than saturated (data points at right in Fig. 14). Also, the zinc partial pressures achieved in tests to date were below the values required to

match the mass flow rate ratios calculated for simulation of the reference engine and in-reactor test unit. The mixed-mean conditions after the addition of cold argon (data points at left in Fig. 14) show a zinc partial pressure two orders of magnitude higher than the saturation partial pressures at corresponding temperature levels; hence, essentially all of the zinc must have been condensed to solid form as the flow progressed down the test section. The test conditions during selected test runs, and brief discussions of the results of the post-test inspections, are listed in Table III.

Photographs of three test sections are shown in Fig. 15. Tube No. 9 is shown as removed from the test section. This tube was tested with radial inflow of the cold gas, a heated tube wall with the wall on the order of 300 K (540 R) above the mixed-mean temperature of the mixture in the test section, and a flow ratio of cold gas to heated vapor/gas mixture of 11.6 to 1. The deposition appeared to be particulate; it was heavy at the inlet end and became lighter with distance down the test section. Subsequent chemical analysis of the deposition on the tube wall indicated that the wall coating was 7.5 percent of the total weight of zinc passed through the tube during the run.

Tube No. 1 (Fig. 15) is shown after attempts to remove the coating from the wall. The test was run with swirling inflow, an unheated wall, and a flow ratio of 2.8 to 1. A considerable amount of the wall deposition was removed by wiping out the inside of the tube, but the first 10 cm downstream of the inlet had a coating which could not be removed. It appeared that this was a plating caused by condensation of vapor directly on the wall.

Tube No. 5 is shown after wiping to remove particulate coatings (Fig. 15). This test was run with swirling inflow, a heated tube wall approximately 200 K (360 R) above the mixed-mean temperature of the vapor/gas mixture, and a flow ratio of 10.2 to 1. Almost all of the material deposited on the wall was removed by wiping with the exception of the local spots which can be seen on the photograph. These spots were probably caused by liquid droplets which contacted the wall before freezing due to turbulence or centrifuging. In tests with similar operating conditions and radial inflow (no swirl on the cold bypass gas), local deposition of this type was not noted.

Figures 16 through 20 are photomicrographs of particle samples taken from the walls of five test sections prior to cleaning. The figures are arranged so that Fig. 16 has the lowest flow ratio of cold gas to heated vapor/gas mixture (2.8 to 1) and the flow ratio increased to 11 to 1 in Fig. 20. The particles formed when the bypass was low (Figs. 16 and 17) were variable in size and had no characteristic shape. As the flow ratio increased, hexagonal crystals were formed. One such crystal may be seen in Fig. 17 with a size on the order of 1.0 micron. As the flow ratio was increased, all of the particles tended to be hexagonal crystals with their sizes decreasing as the flow ratio increased. It is believed that the particles noted at low flow ratios (Figs. 16 and 17) were part of a film formed by vapor or liquid contacting the wall, but the crystalline particles are those which solidified in the stream. Comparison of the samples taken from the inlet and outlet ends of the test section showed a trend of larger particles and agglomerates at the outlet.

Effects of Heating Tube Walls

Heating of the tube walls to produce temperature differentials as high as 300 K (540 R) did not have any appreciable effect in the zinc/argon tests. In some of the tests with very high wall temperatures, there was a decrease in the amount of particulate coating near the downstream end of the test section. It is believed that this was due to the increase in local velocity near the wall (and, hence, scrubbing) caused by the heat addition, rather than due to revaporization of the material on the wall. Further tests should be performed to verify this hypothesis.

Effects of Inlet Geometry

No appreciable differences were noted between the tests with swirling inflow and those with radial inflow. The angular momentum of the vapor/gas mixture leaving the vaporizer section in tests with swirling inflow was probably small relative to that of the bypass flow at injection. The argon at the base of the plasma torch was injected at an angle of only 3 degrees from radial direction. This gave a tangential velocity component equal to about 5 percent of the injection velocity. The injection geometry for swirling inflow could not be varied to produce different amounts of swirl velocity. This would be necessary for a more definitive analysis of the swirl effects. No zinc accumulation was noted in the inlet region with either inlet geometry.

RECOMMENDATIONS FOR FURTHER EXPERIMENTS

The experiments discussed herein were preliminary in nature. The conclusions which have been drawn should be verified by additional experiments in the same operating range, with concentration of effort on more detailed measurements of the particle size, amount of wall coating, velocity distributions, and temperature distributions within the duct and at the duct wall. These experiments should concentrate on zinc/argon or other metal-vapor/gas systems, rather than on the iodine/air system, since the operating conditions in the metal-vapor/gas systems more closely simulate the reference engine and in-reactor test unit. In addition to further tests with the zinc/argon system, investigations should be made with additional vapor/gas systems, additional duct inlet and exit geometries, and with attachments which will permit separation of the particles and gas.

Investigation of Other Vapor/Gas Mixtures

Since the iodine/air experiments and zinc/argon experiments were not suitable for cross-correlation, it is suggested that additional experiments be performed with metals other than zinc. Inspection of Fig. 4 shows that cadmium, antimony and bismuth are the closest to zinc in the temperature levels required to provide the required partial pressure. One additional factor which should be considered in the selection of the material to be used is the surface tension. It is believed that the primary reason for the great difference in size between the iodine particles and the zinc particles is, in part, due to the surface tension. Although no published data on the surface tension of iodine was found in the literature, if the surface tension is approximated using Eotvos' equation (Ref. 7) it is found to be on the order of 57 dynes/cm. The surface tension of zinc is between 760 and 780 dynes/cm (Ref. 8). The equations used in the calculation of droplet radius in an evaporization or condensation process (see Ref. 9) indicate that the droplet radius is inversely proportional to the surface tension. The surface tension of uranium was also not found in the literature, but it was calculated according to the approximation equation previously mentioned, to be on the order of 1000 to 1200 dynes/cm. Of the material listed on Fig. 4, the ranges of surface tension are, in dynes/cm: zinc, 760-780; cadmium, 580-600; tin, 500-520; antimony, lead and bismuth, 320-400 (Ref. 8). Thus, zinc seems to be the best for simulating uranium; however, tests with other metals should be conducted for confirmation of the effect of surface tension on particle size.

Investigation of Additional Duct Geometries

Further investigations of the effects of inlet geometry should be made, particularly with regard to the requirement to swirl the bypass flow. In the reference engine and the in-reactor test unit, the flow exiting the cavity will have swirl. The exact magnitude of the rotational velocity is at present unknown. However, it is probably reasonable to assume that the flow entering the exhaust port will rotate as a solid body with a rotational velocity, at a radius equal to the exhaust duct radius, which is at least equal to the rotational velocity

in the buffer-gas region. The amount of swirl in the exhaust duct region of the reference engine and in-reactor test unit would then depend upon both the rotational velocity in the buffer-gas region and the exhaust port diameter.

The rotational velocity in the bypass flow may be controlled by varying the injection angle. To produce a stable swirling flow in the exhaust port, the angular momentum of the bypass must be greater than that of the exhaust flow. Additional experiments should be conducted to determine if it is better to promote stability with high angular momentum in the bypass or to break up the exhaust flow and promote mixing. In the preliminary tests, no appreciable differences were noted between tests with swirling inflow and those with radial inflow. An injection geometry with variable inlets capable of producing different angular momentum at a constant mass flow rate should be fabricated to investigate this effect in future tests.

The particulate coating noted in the zinc/argon tests must also be avoided. Even though the percentage of the total metal flow which adheres to the wall is relatively low, accumulations of uranium in the exhaust ports would represent a considerable heat source due to continued fissioning of the uranium. It is probable that particulate deposition can be reduced by the addition of a particle-free buffer gas in the boundary layer of the tube using methods similar to those used for minimizing the deposition of propellant seed particles in the propellant heating duct. A sketch of a proposed exhaust duct configuration incorporating a radial inflow geometry using porous-wall tubes and boundary layer injection of cold gas is shown in Fig. 21. Actual duct sizes required have not been calculated. Additional experiments should be conducted with this type of geometry prior to performing a detailed design of the exhaust system.

A means for controlling the test section pressure level, such as an outlet valve, should also be incorporated to permit operation at pressures above 1 atm.

Investigation of Separator Requirements

As a part of the investigation of different duct exit geometries, it would be desirable to design and test devices which would separate the particles and the gas. More information with regard to particle size and particle distribution is necessary to define the types of separation methods that could be used effectively; the most desirable methods would employ devices which would concentrate the particles by flow control, such as a centrifugal separator.

REFERENCES

1. McLafferty, G. H. and H. E. Bauer: Studies of Specific Nuclear Light Bulb and Open-Cycle Vortex-Stabilized Gaseous Nuclear Rocket Engines. United Aircraft Research Laboratories Report G-910093-37, prepared under Contract NASw-847, September 1967. Also issued as NASA CR-1030.

2. Bauer, H. E., R. J. Rodgers and T. S. Latham: Analytical Studies of Start-Up and Dynamic Response Characteristics of the Nuclear Light Bulb Engine. United Aircraft Research Laboratories Report J-910900-5, prepared under Contract SNPC-70, September 1970. Also issued as NASA CR-111097.

3. Latham, T. S. and H. E. Bauer: Analytical Design Studies of In-Reactor Tests of a Nuclear Light Bulb Unit Cell. United Aircraft Research Laboratories Report K-910900-11, prepared under Contract SNPC-70, September 1971.

4. Roman, W. C. and J. F. Jaminet: Experimental Investigations to Simulate the Thermal Environment and Fuel Region in Nuclear Light Bulb Reactors using an R-F Radiant Energy Source. United Aircraft Research Laboratories Report K-910900-7, prepared under Contract SNPC-70, September 1971.

5. Klein, J. F.: Experiments to Simulate Heating of Propellant by Thermal Radiation in a Nuclear Light Bulb Engine. United Aircraft Research Laboratories Report K-910900-8, prepared under Contract SNPC-70, September 1971.

6. McLafferty, G. H.: Investigation of Gaseous Nuclear Rocket Technology - Summary Technical Report. United Aircraft Research Laboratories Report H-910093-46, prepared under Contract NASw-847, November 1969.

7. Perry, J. H., editor: Chemical Engineers Handbook. Third Edition, McGraw-Hill Book Company Inc., New York, 1962.

8. Weast, R. C., editor: Handbook of Chemistry and Physics. 49th Edition, The Chemical Rubber Co., Cleveland, Ohio, 1968.

9. Fuchs, N. A.: Evaporation and Droplet Growth in Gaseous Media. Pergammon Press, New York, 1959.

LIST OF SYMBOLS

d	Diameter, cm or in.
h	Convective heat transfer coefficient, kw/cm or Btu/sec-ft
k	Thermal conductivity, kw/cm or Btu/sec-ft
m_g	Molecular weight of gas in vapor/gas mixture, gm or lb
m_v	Molecular weight of vapor in vapor/gas mixture, gm or lb
m_x	Molecular weight of x component of gas mixture, gm or lb
m_y	Molecular weight of y component of gas mixture, gm or lb
P_F	Partial pressure of fuel (uranium), atm
P_g	Partial pressure of gas in vapor/gas mixture, atm
P_I	Partial pressure of iodine in iodine/air mixture, atm
P_t	Total pressure, atm
P_v	Partial pressure of vapor in vapor/gas mixture, atm
P_x	Partial pressure of x component of gas mixture, atm
P_y	Partial pressure of y component of gas mixture, atm
P_Z	Partial pressure of zinc in zinc/argon mixture, atm
Pr	Prandtl number
Re	Reynolds number
T_m	Mixed-mean temperature, deg K or deg R
T_w	Wall temperature, deg K or deg R
w_g	Mass flow rate of gas in vapor/gas mixture, gm/sec or lb/sec
w_v	Mass flow rate of vapor in vapor/gas mixture, gm/sec or lb/sec

TABLE I

FUEL AND BUFFER-GAS OUTFLOW CONDITIONS FOR REFERENCE ENGINE AND IN-REACTOR TEST UNIT CELL

	In-Reactor Test	Reference Engine Unit Cavity
Fuel Flow Rate, gm/sec (lb/sec)	1.59 (3.5×10^{-3})	485.0 (1.07)
Fuel Carrier-Gas Flow Rate, gm/sec (lb/sec)	0.265 (5.84×10^{-4})	81.5 (0.179)
Buffer-Gas Flow Rate, gm/sec (lb/sec)	25.3 (5.6×10^{-2})	1590 (3.50)
Total Outflow, gm/sec (lb/sec)	27.1 (6.0×10^{-2})	2156 (4.75)
Exit Temperature of Outflow from Cavity, deg K (deg R)	4800 (8640)	6550 (11,800)
Fuel-to-Gas Mass Flow Rate Ratio	0.0628	0.29
Uranium Partial Pressure, atm	5.2	12
Calculated Bypass Flow, gm/sec (lb/sec)*	36.2 (0.08)	8000 (17.6)

*Bypass flow requirement based on quantity of cold gas necessary to reduce the mixed-mean temperature of the mixture of exhaust flow and bypass to 1390 K (2500 R).

TABLE II

SUMMARY OF SELECTED DATA FROM IODINE/AIR TESTS

Data Plotted In Fig. 8

Run No.	Flow Ratio[2]	Iodine Partial Pressure After Mixing, atm	Mixture Temperature, deg K		Wall Temperature Difference, deg K[5]
			Inlet[3]	Outlet[4]	
11[1]	13.3	0.0094	301	326	22
12	8.2	0.0146	307	327	16
13	6.6	0.0171	309	330	15
14	4.2	0.022	312	335	11
15	2.8	0.0339	338	347	9
16	2.65	0.0398	341	354	8
21[1]	19.4	0.00464	299	317	16
22	18.6	0.00565	304	318	13
23	14.7	0.00705	310	321	11
24	13.2	0.00780	313	323	9

(1) The iodine partial pressure of the iodine/air mixture entering the test section was held constant during each test series. The iodine partial pressure was 0.126 atm in tests 11 through 16 and 0.072 atm in tests 21 through 24.

(2) Mass flow ratio of cold bypass gas to heated vapor/gas mixture.

(3) Calculated mixed-mean temperature after addition of cold gas.

(4) Measured temperature at test section outlet.

(5) Difference between mixed-mean temperature and test section wall temperature.

TABLE III

SUMMARY OF SELECTED DATA FROM ZINC/ARGON TESTS

(a) Operating Conditions

Test No.	Flow Ratio(1)	Run Time, min	Zinc Partial Pressure, atm		Mixture Temperature, deg K		
			Vaporizer	Test Section	Vaporizer(2)	Inlet(3)	Outlet(4)
1	2.8	3.5	0.000435	0.000088	--	--	483
2	3.4	3.0	0.000645	0.000123	1190	496	520
3	6.2	3.5	0.00153	0.000185	1080	402	496
4	11.0	4.0	0.00131	0.0000916	958	345	429
5	10.2	9.0	0.0040	0.000304	1176	369	431
9	11.6	2.0	0.00865	0.000586	958	342	445
10	12.5	3.0	0.01269	0.000801	1080	347	334
11	9.5	3.0	0.0141	0.00115	1152	371	357
12	6.8	4.0	0.0141	0.00153	1235	409	380
13	12.5	3.5	0.0155	0.00098	1291	363	356
14	9.5	3.0	0.0121	0.00815	1266	381	364
16	12.5	4.0	0.007	0.0047	1251	362	356

(1) Mass flow ratio of cold bypass gas to heated vapor/gas mixture
(2) Temperature of vapor/gas mixture exiting vaporizer (measured).
(3) Calculated mixed-mean temperature after addition of cold gas.
(4) Measured outlet temperature. Higher than mixed-mean for cases with heated walls, lower than mixed-mean for cases with unheated walls.

TABLE III (Continued)

(b) Post-Test Inspection Results

Test No.	Test Conditions(1)	Appearance After Test		Particle Size, Microns	
		Before Wiping	After Wiping	Inlet	Outlet
1	U-S	Coated Entire Length	Plating First 10-12 cm	1-2	1-2
2	H-S	Coated Entire Length	Plating First 8-10 cm	1-2	1-2
3	H-S	Coated Entire Length	Plating First 6-8 cm	0.3-0.5	1-2
4	H-S	Coated Entire Length	Light Plating Entire Length	0.05-0.1	0.2-0.4
5	H-S	Coated Entire Length	Plating in Spots(2)	0.05-0.10	0.1-0.3
9	H-S	Coated First 25-30 cm(2)	See Note (3)		
10	U-R	Coated Entire Length	Clean Entire Length		
11	U-R	Coated Entire Length	Light Plating First 5 cm		
12	U-R	Coated Entire Length	Plating First 8 cm		
13	U-S	Coated Entire Length	Plating First 5 cm		
14	U-S	Coated Entire Length	Light Plating Entire Length		
16	U-R	Coated Entire Length	See Note (3)		

(1) U - Unheated Tube Wall, H - Heated Tube Wall, S - Swirling Inflow, R - Radial Inflow.
(2) Tubes shown in Fig. 15.
(3) Coating removed with hydrochloric acid to measure total quantity of zinc on wall. Results indicate 7.5 percent of total mass of zinc flowing through tube in tube No. 9, 2.6 percent in tube No. 16.

K-910900-9

FIG. 1

NUCLEAR LIGHT BULB FLOW DIAGRAM

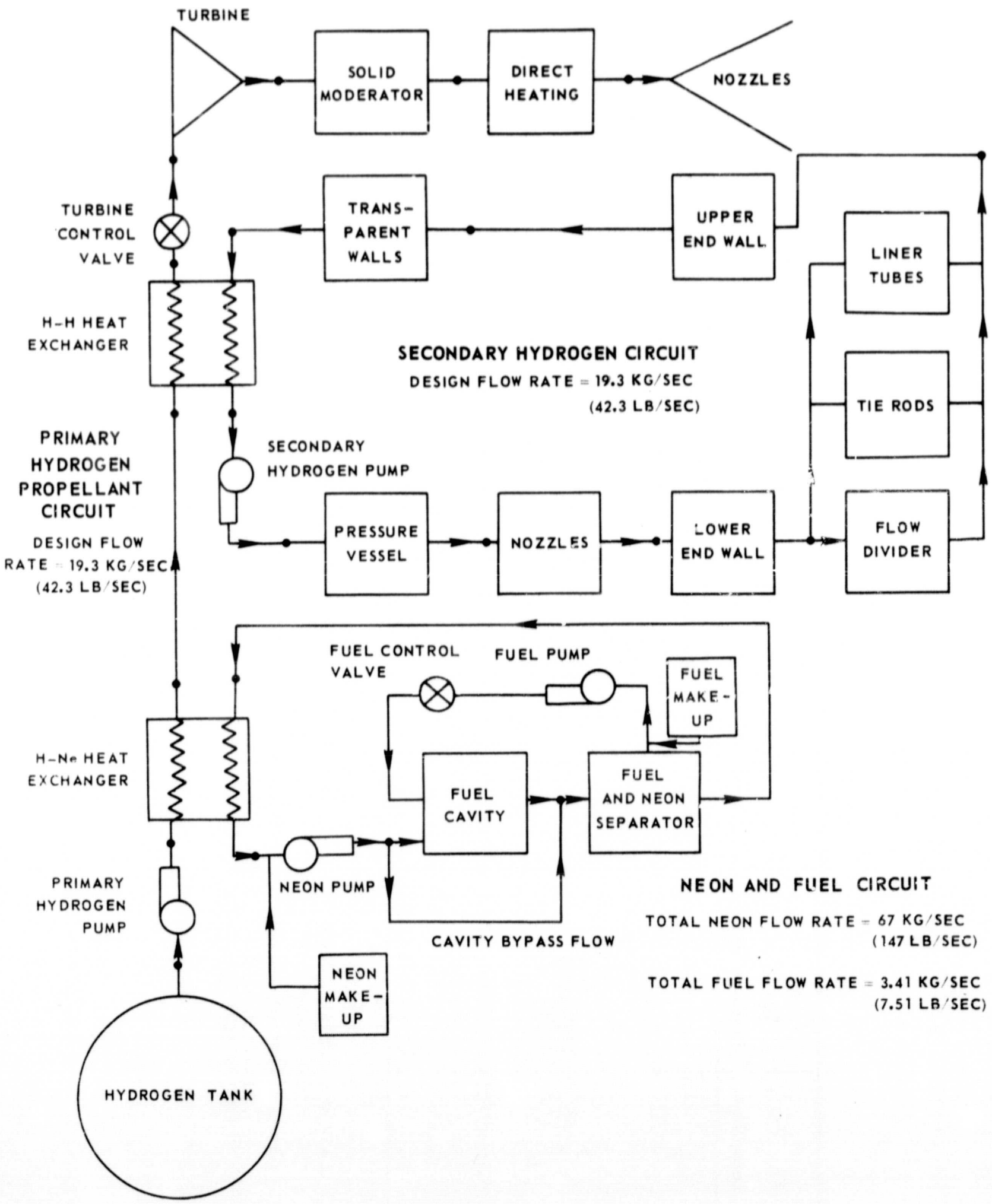

K-910900-9

FIG. 2

BASIC CONFIGURATION OF IN-REACTOR TEST UNIT CELL

TEST CELL LENGTH = 17.8 CM (7.0 IN.) BETWEEN END WALLS

(a) SECTION A-A

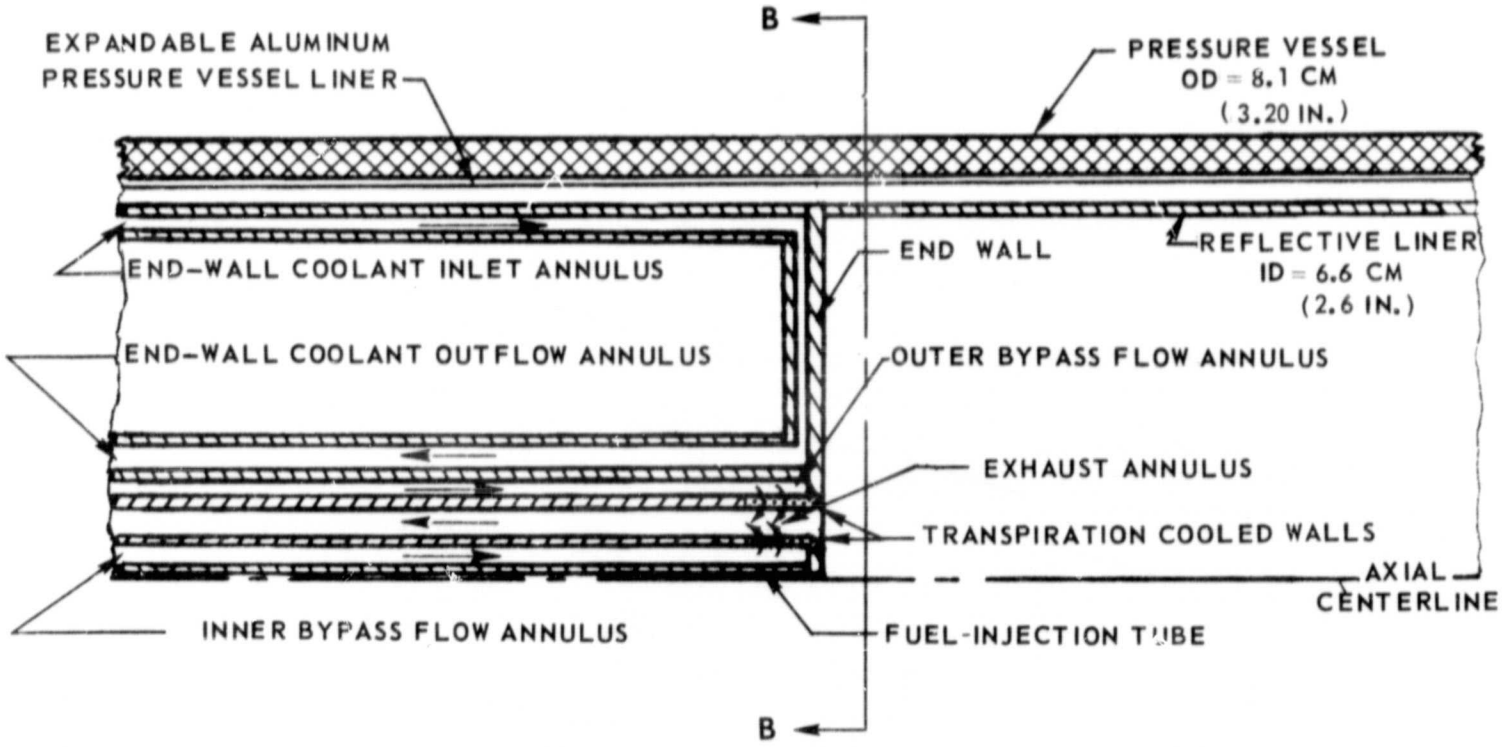

(b) SECTION B-B

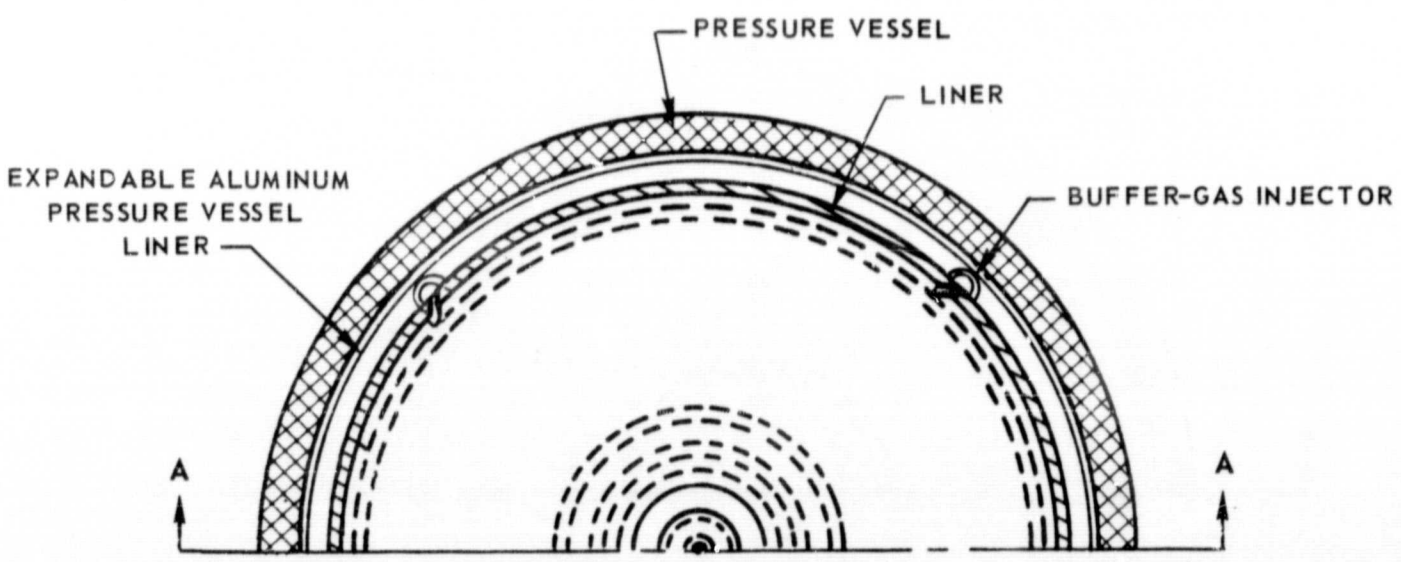

FIG. 3

IN-REACTOR TEST UNIT CELL WITH OFF-CENTER FUEL INJECTION PORT

TEST CELL LENGTH = 17.8 CM (7.0 IN.) BETWEEN END WALLS

(a) SECTION A-A

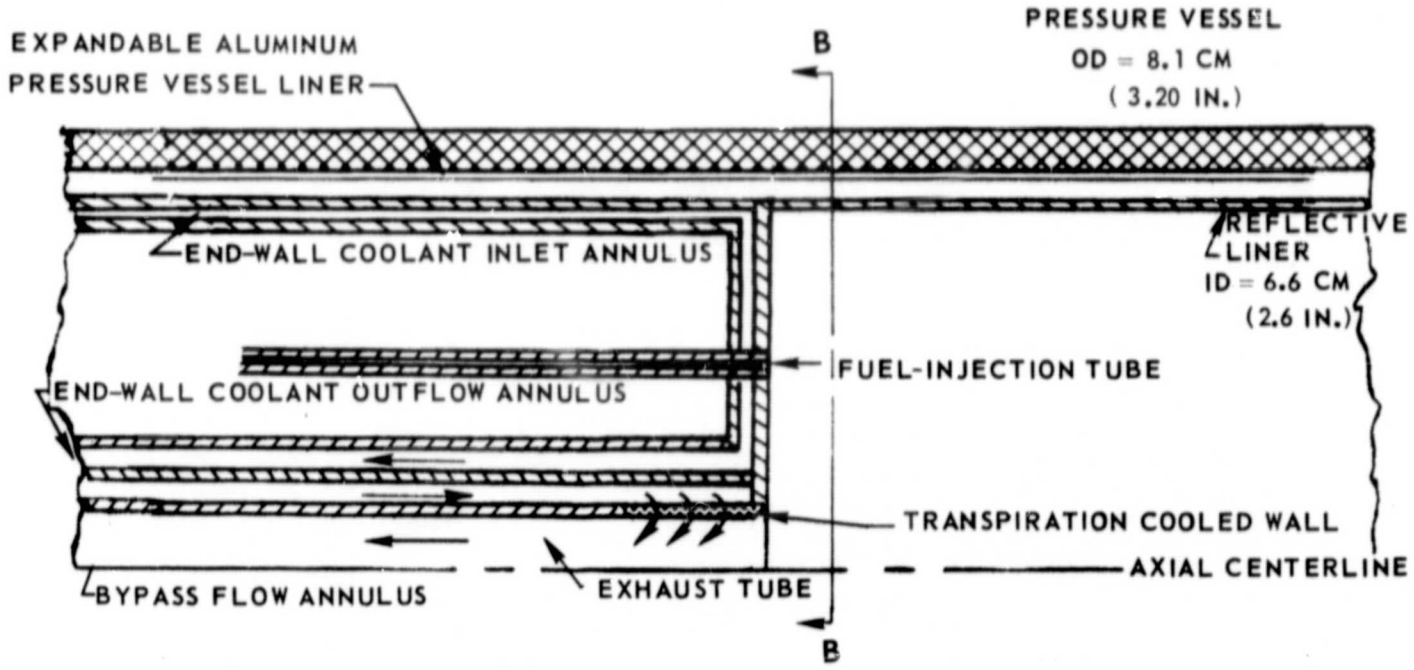

(b) SECTION B-B

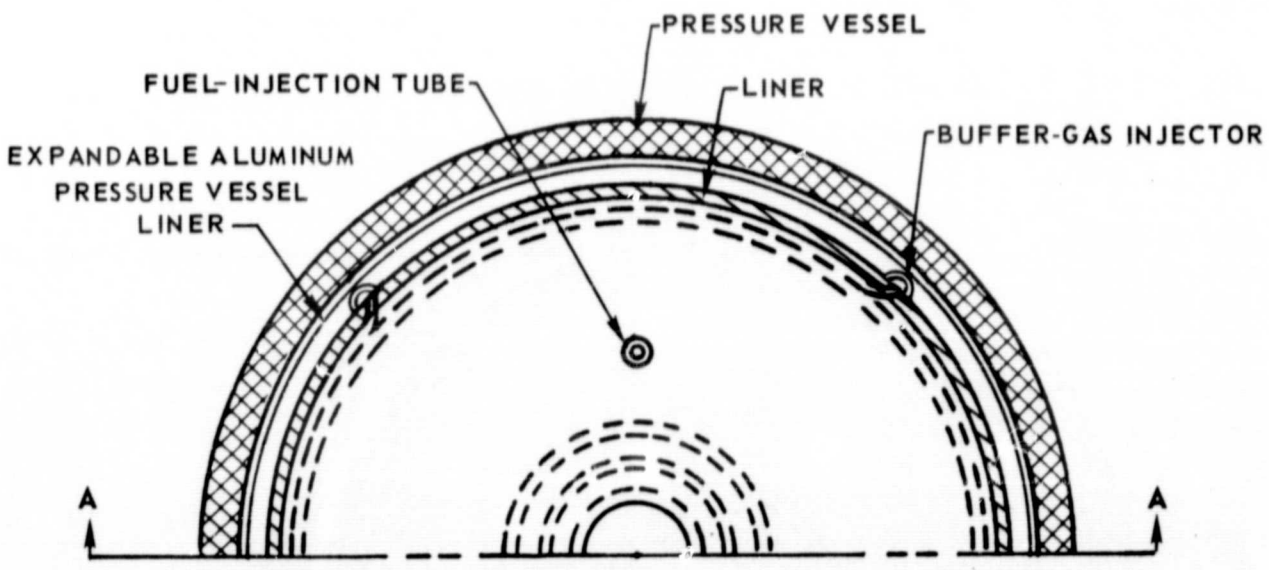

FIG. 4

VAPOR PRESSURES OF MATERIALS CONSIDERED FOR USE IN CONDENSATION TESTS

SYMBOLS DENOTE CONDITIONS REQUIRED IN VAPORIZER AT 1 ATM TO MATCH MASS FLOW RATE IN REFERENCE ENGINE

□ ARGON GAS ○ HELIUM GAS △ AIR (USED WITH IODINE ONLY)

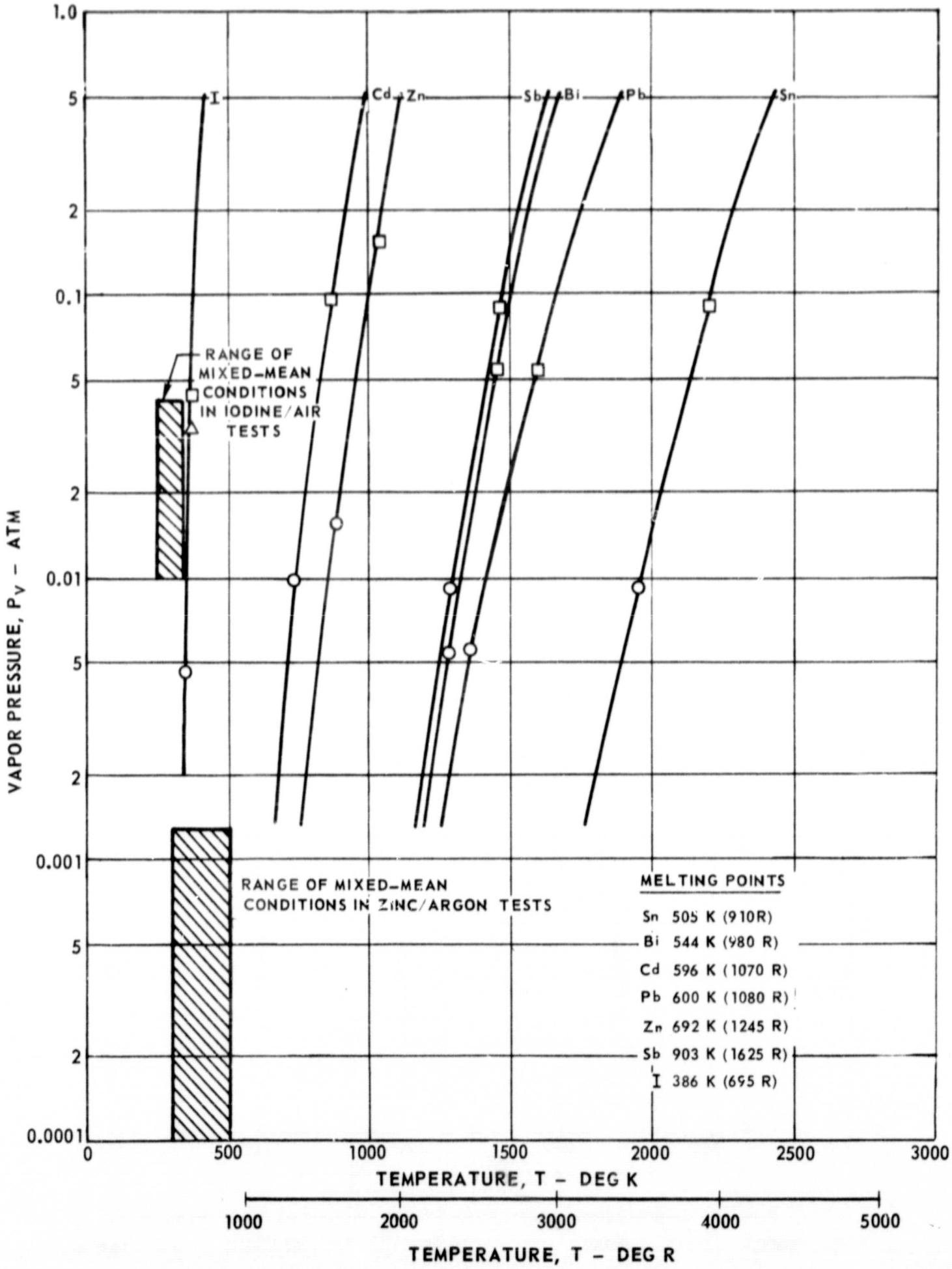

FIG. 5

VAPOR PRESSURE OF URANIUM AND PARTIAL PRESSURE AND TEMPERATURE CONDITIONS EXPECTED IN REFERENCE ENGINE AND IN-REACTOR TEST UNIT CELL

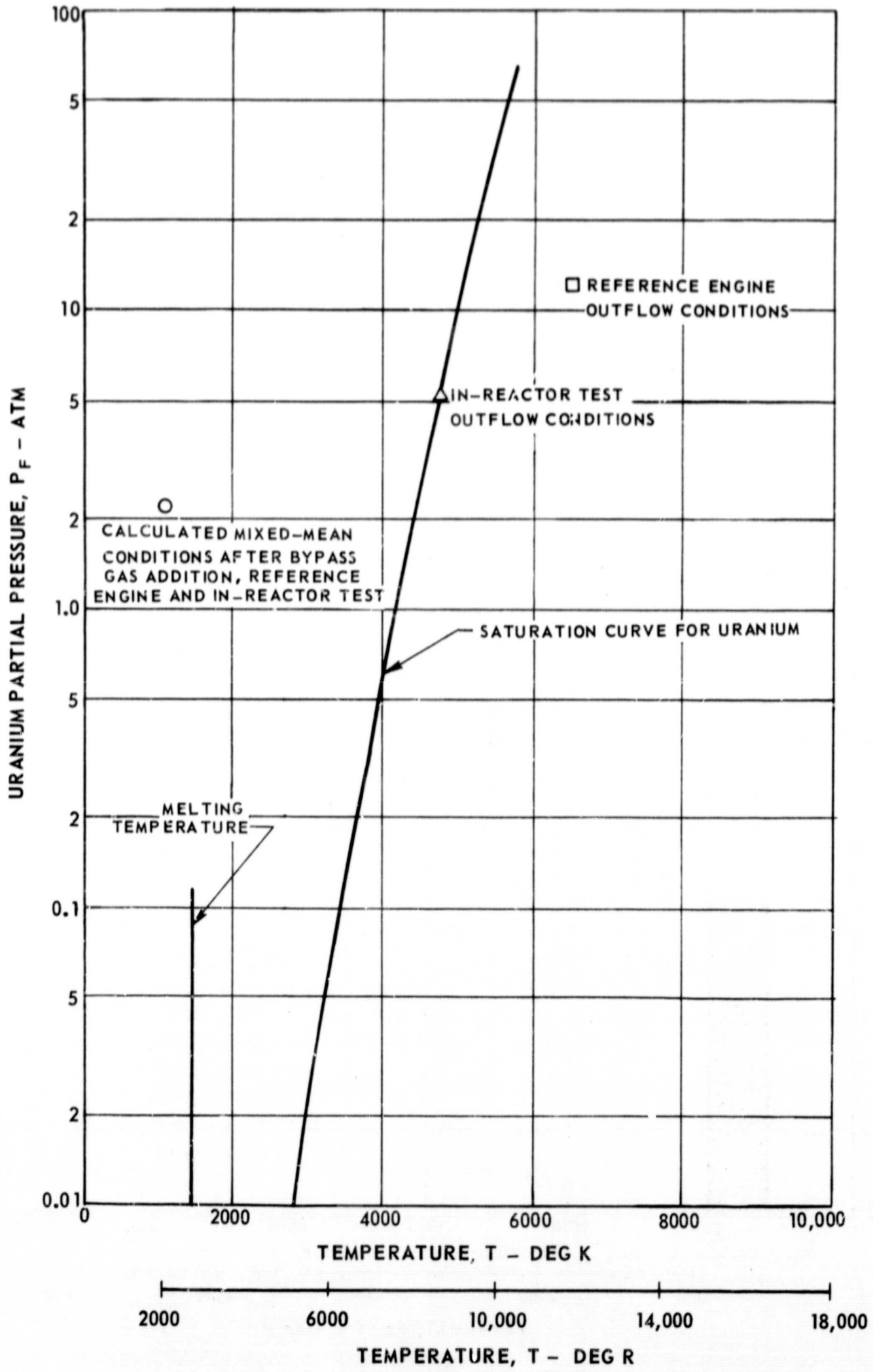

FIG. 6

SKETCH OF TEST EQUIPMENT FOR IODINE/AIR TESTS

SEE FIG. 7 FOR SWIRLING FLOW INLET CONFIGURATION

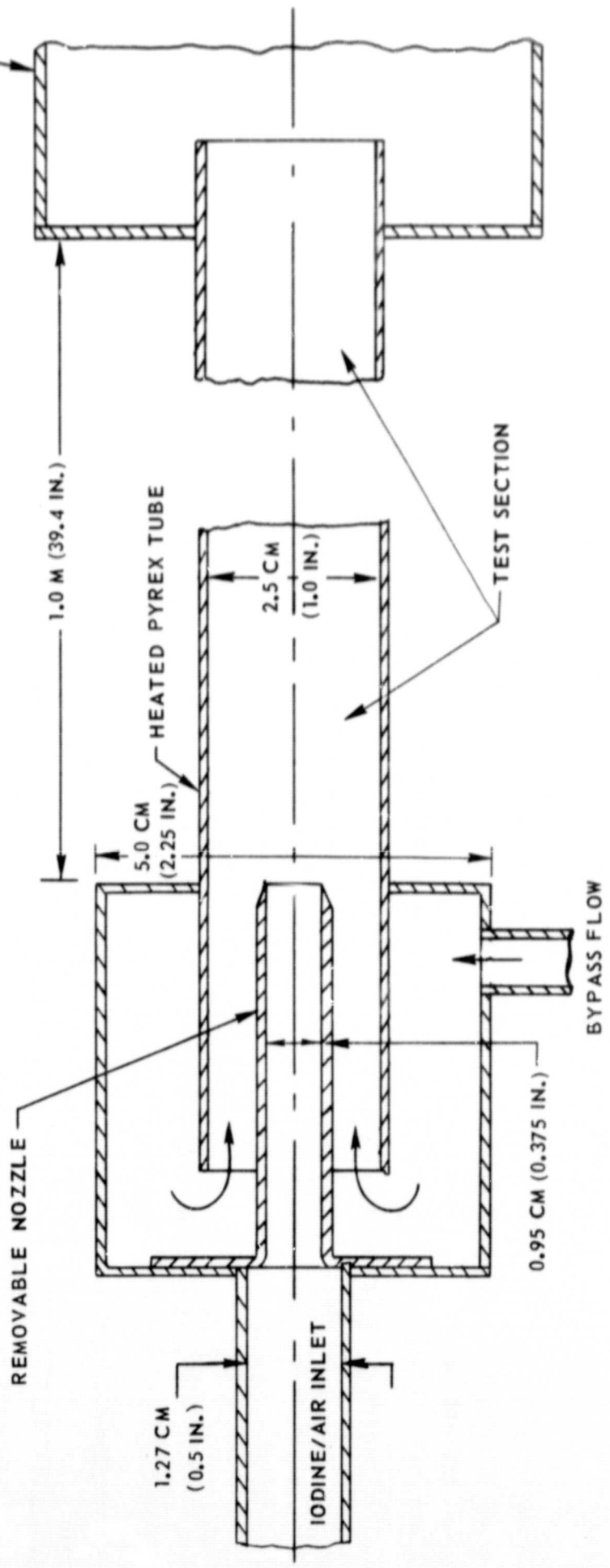

SKETCH OF SWIRLING FLOW INLET CONFIGURATION FOR IODINE/AIR TESTS

SEE FIG. 6 FOR INLET CONFIGURATION WITHOUT SWIRLING FLOW

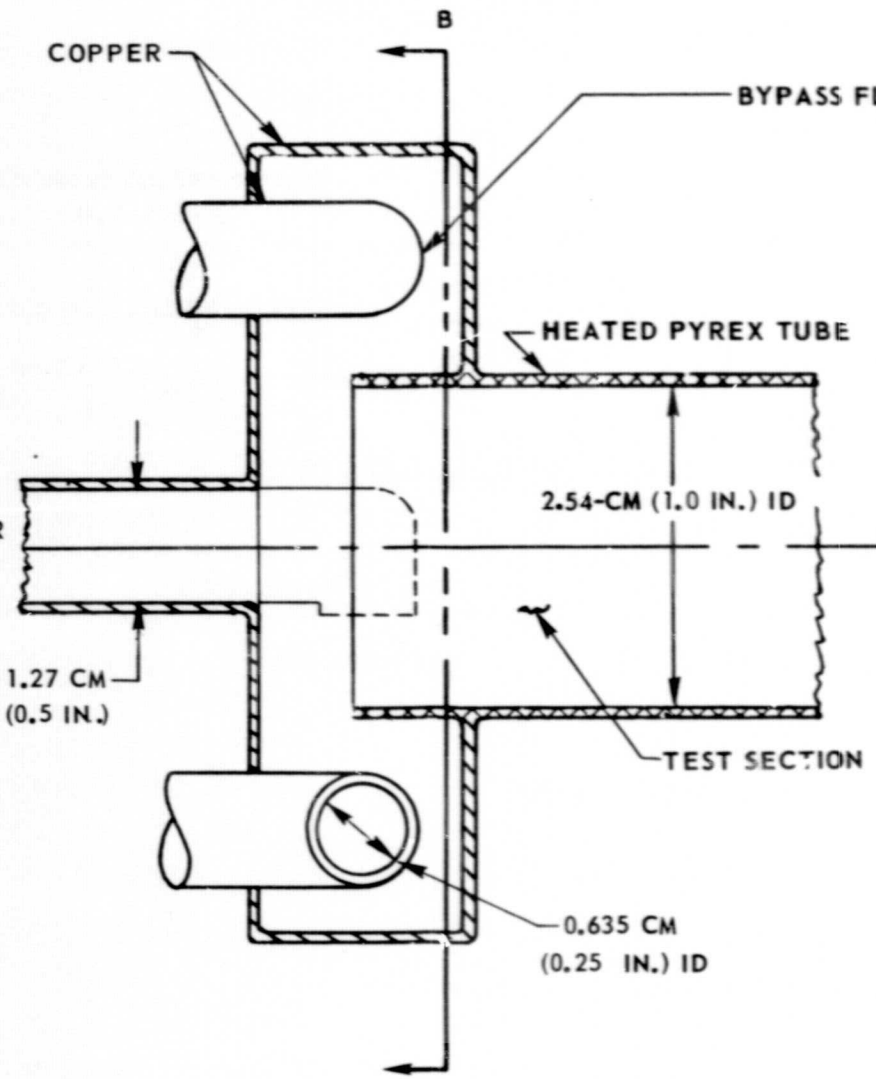

SECTION A–A

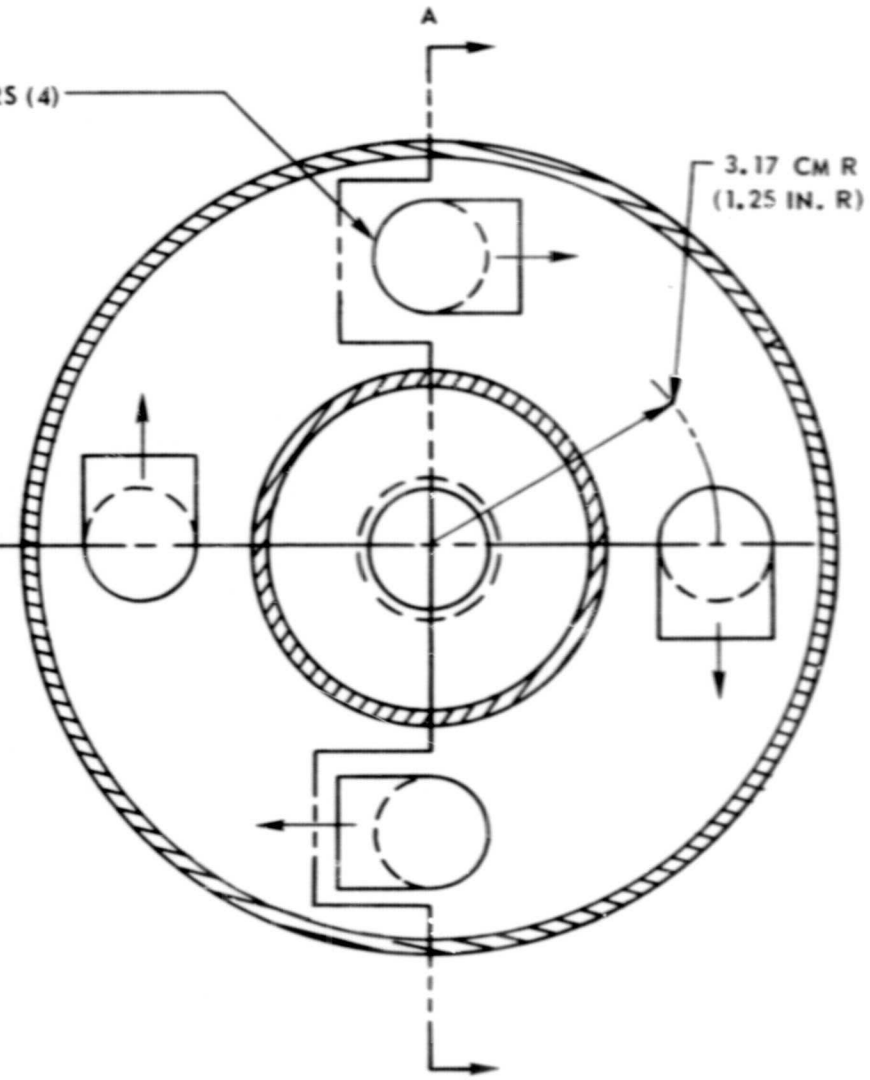

SECTION B–B

FIG. 7

FIG. 8

RESULTS OF IODINE/AIR TESTS WITH HEATED TUBE WALLS

SEE FIGS. 6 AND 7 FOR TEST EQUIPMENT

NUMBERS DENOTE TEST CONDITIONS IN TABLE II

CLOSED SYMBOLS – BYPASS FLOW INJECTED WITH SWIRL

OPEN SYMBOLS – BYPASS FLOW INJECTED WITHOUT SWIRL

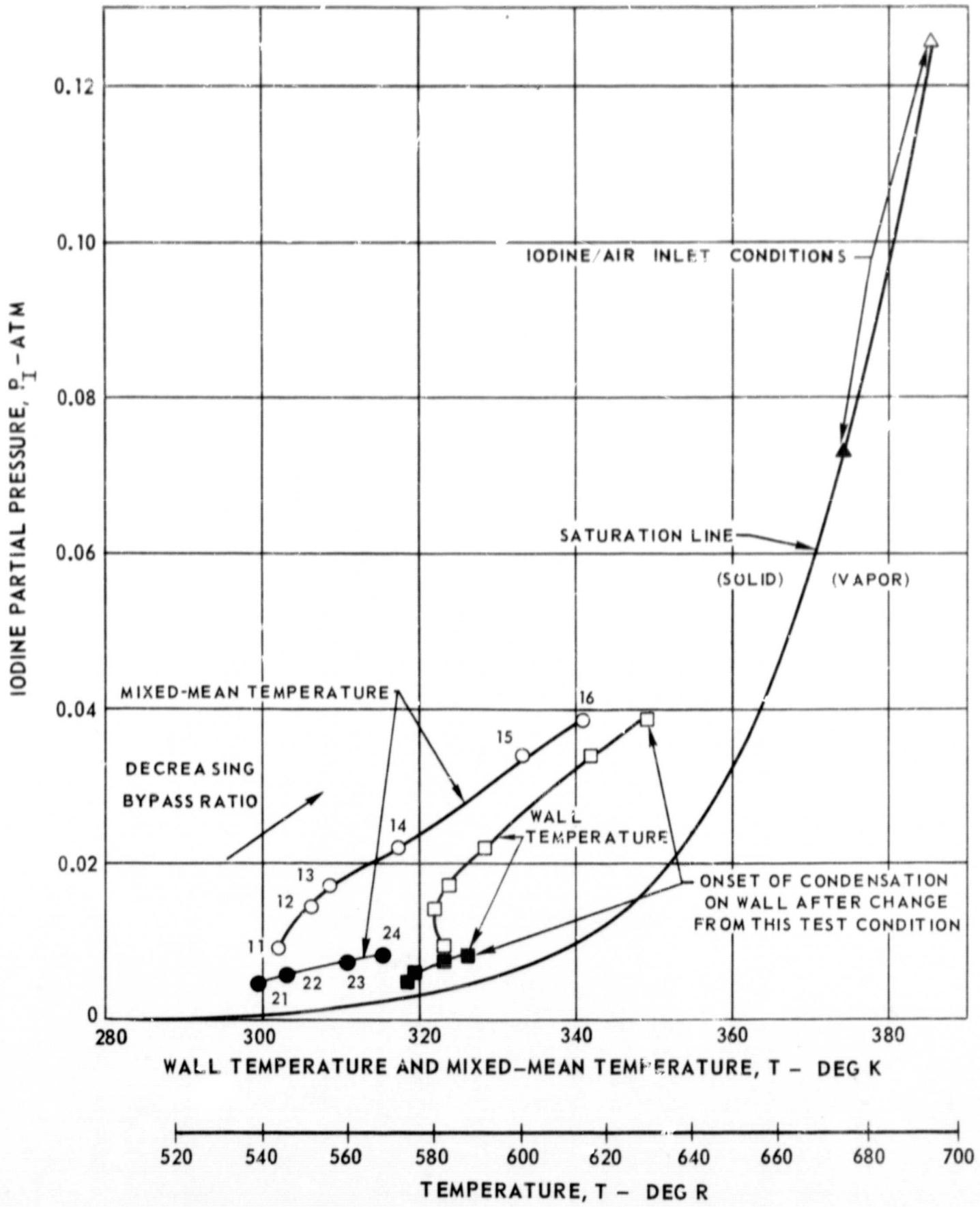

FIG. 9

SKETCH OF EQUIPMENT FOR ZINC/ARGON TESTS

INLETS WITH AND WITHOUT SWIRL USED (SEE FIGS. 12 AND 13 FOR INLET GEOMETRIES)

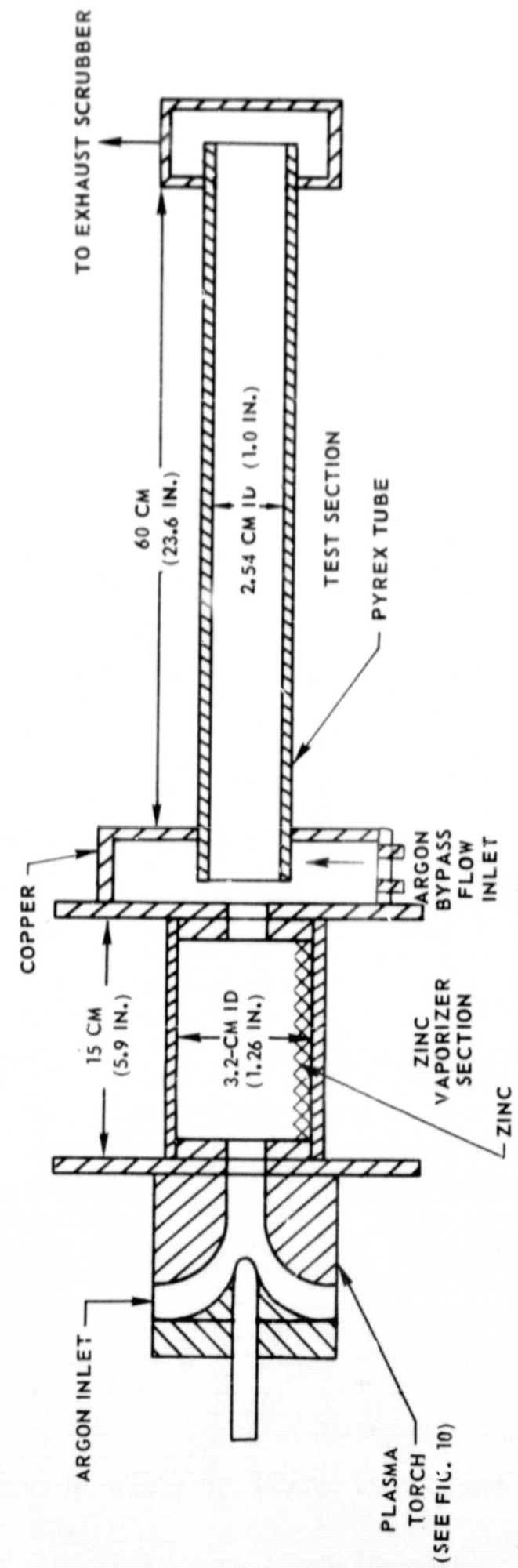

FIG. 10

PHOTOGRAPH OF EQUIPMENT FOR ZINC/ARGON TESTS

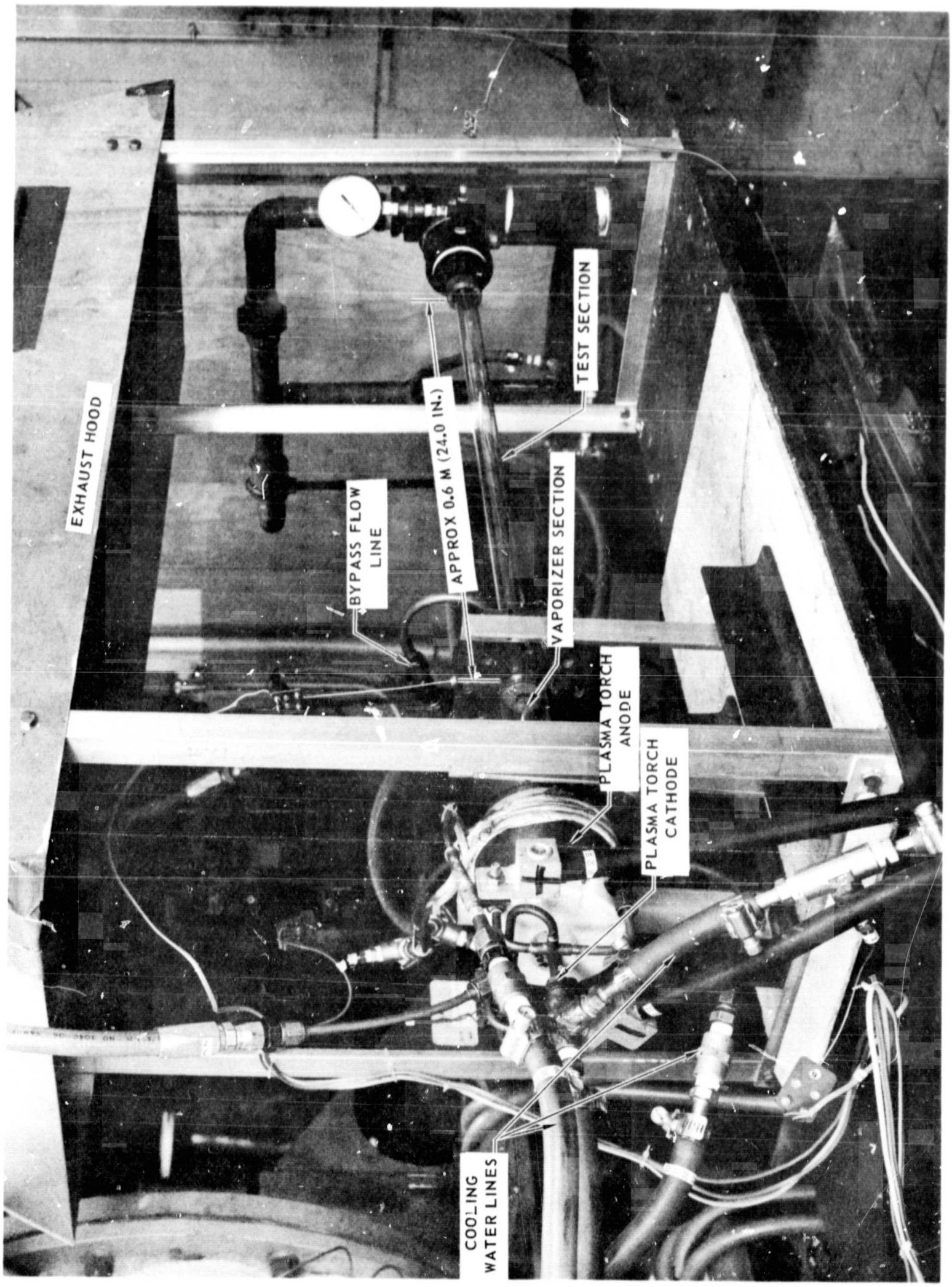

K-910900-9

FIG. 11

D-C ARC PLASMA TORCH USED IN ZINC/ARGON TESTS

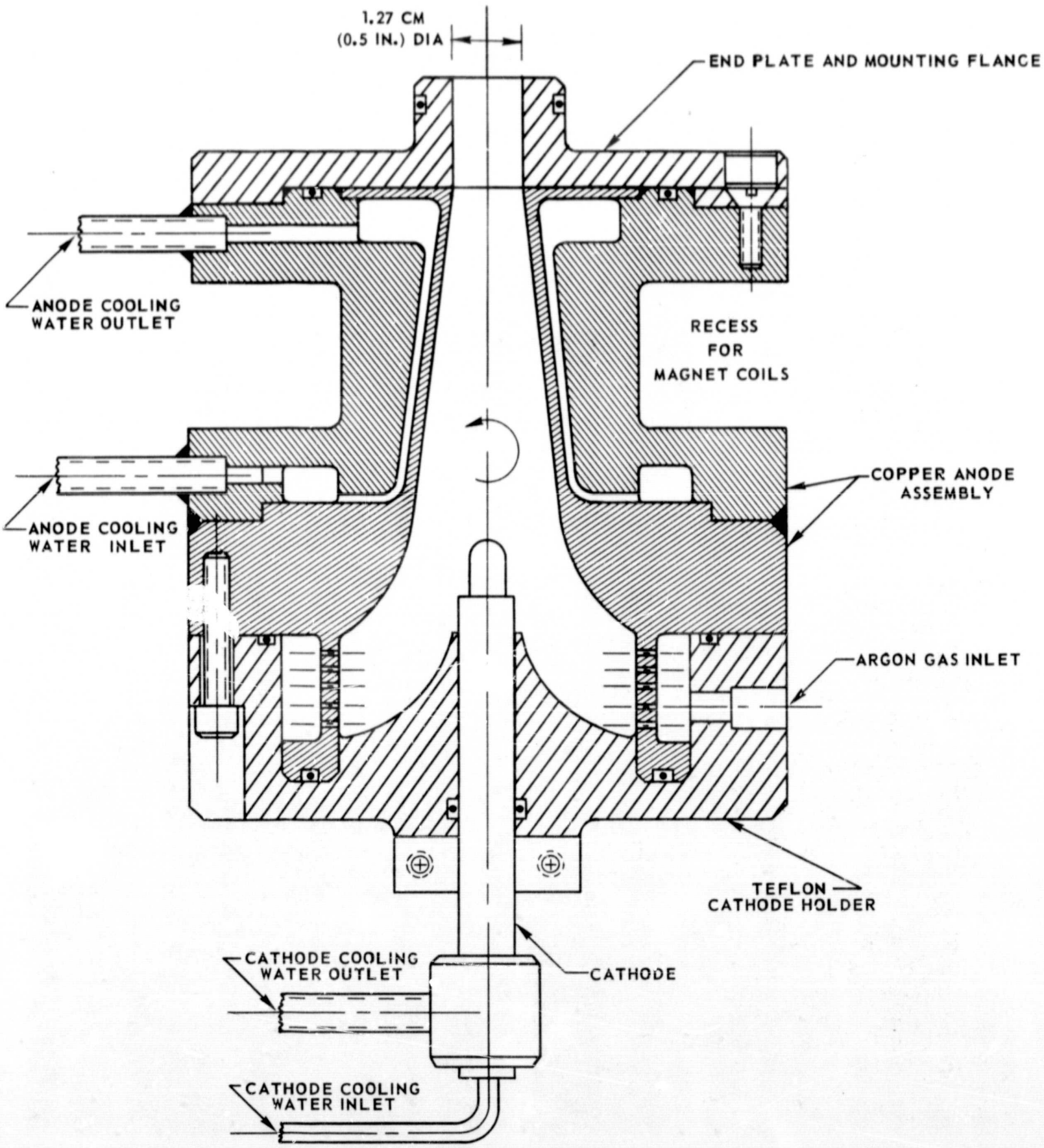

K-910900-9

FIG. 12

PHOTOGRAPH OF BYPASS FLOW INLET WITH SWIRLING FLOW CONFIGURATION

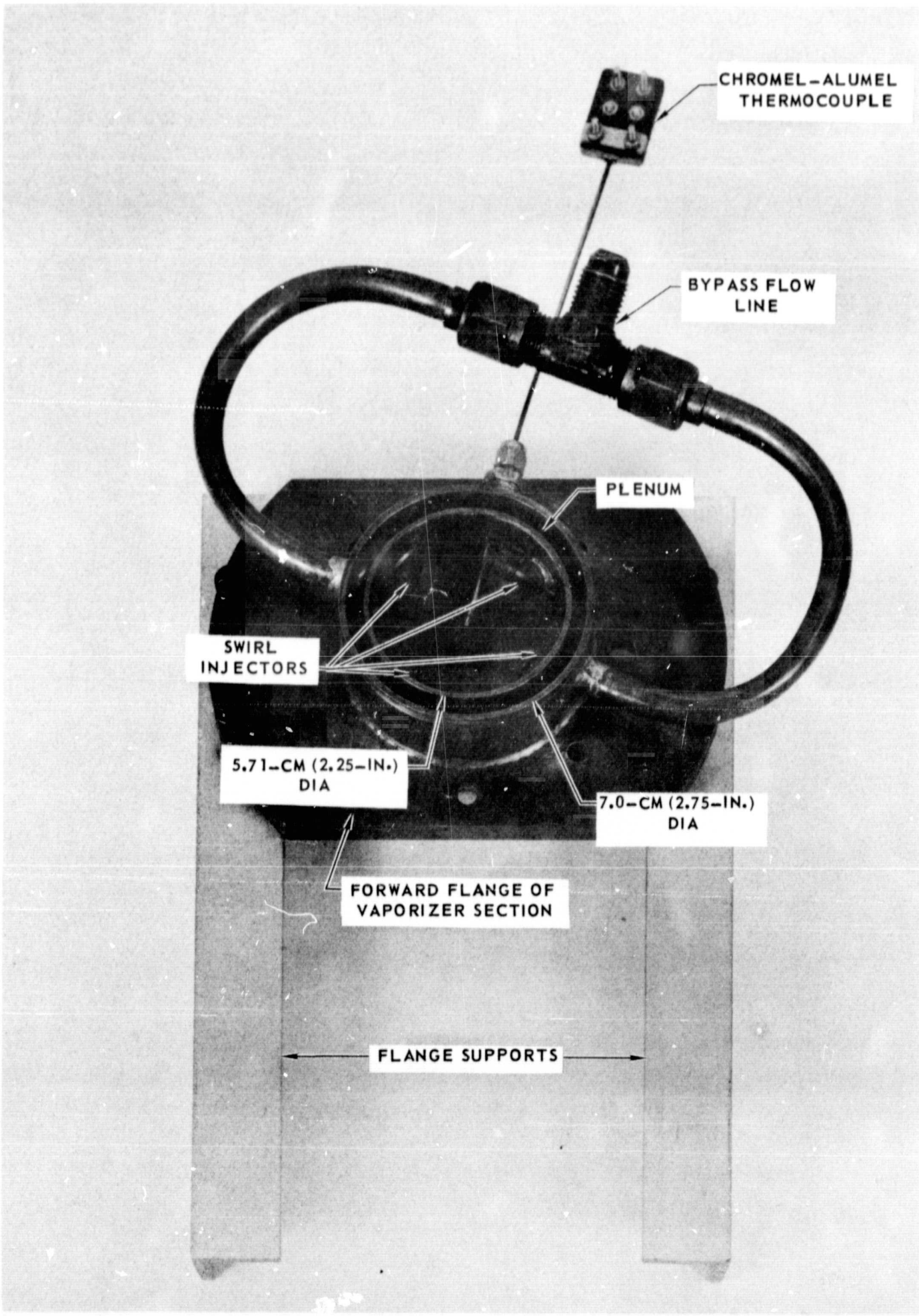

K-910900-9

FIG. 13

PHOTOGRAPH OF BYPASS FLOW INLET WITH RADIAL INFLOW CONFIGURATION

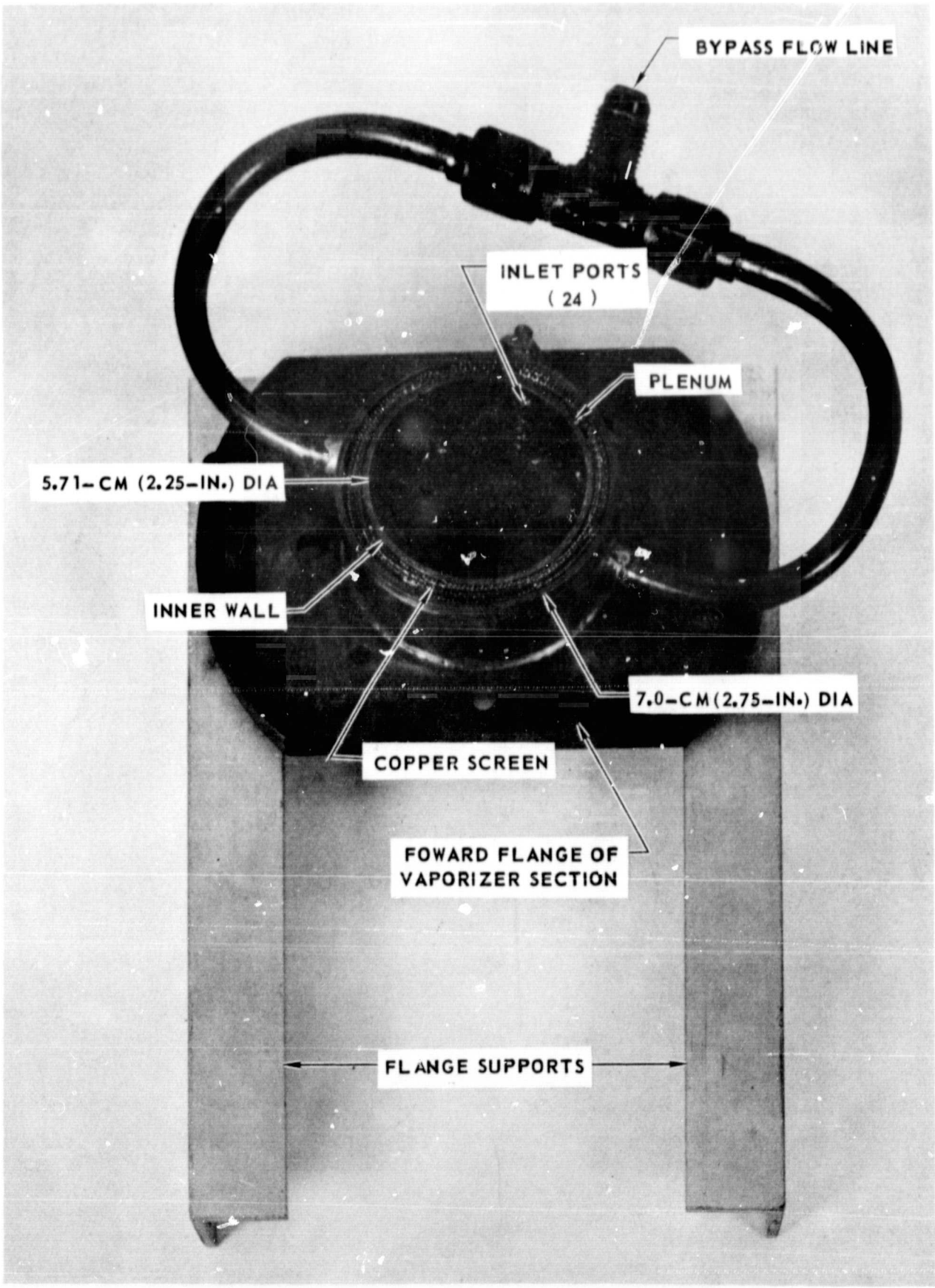

K-910900-9

FIG. 14

TEST CONDITIONS FOR ZINC-ARGON EXPERIMENTS

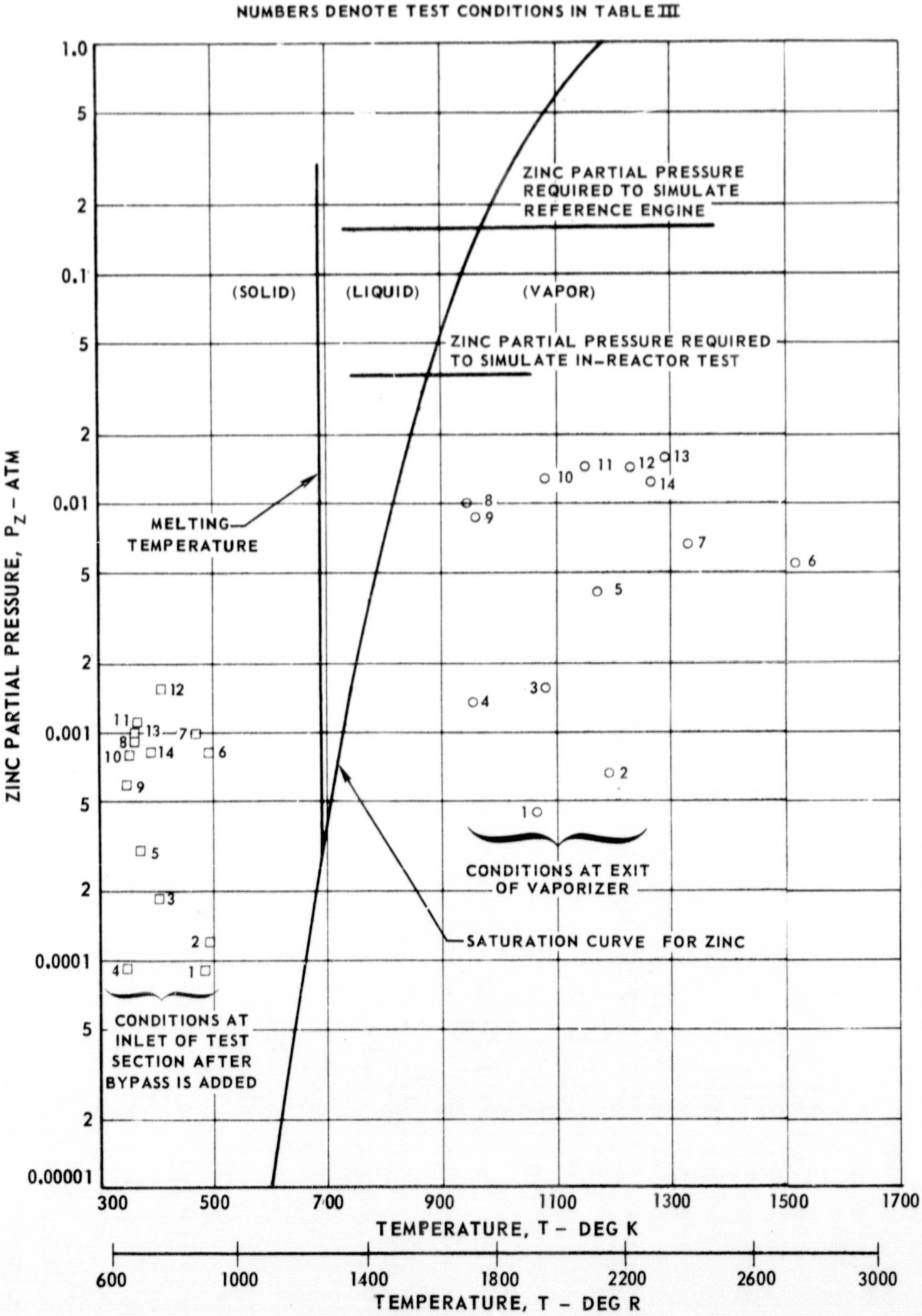

FIG. 15

TEST SECTION TUBES AFTER OPERATION

SEE TEXT AND TABLE III FOR DESCRIPTION OF OPERATING CONDITIONS

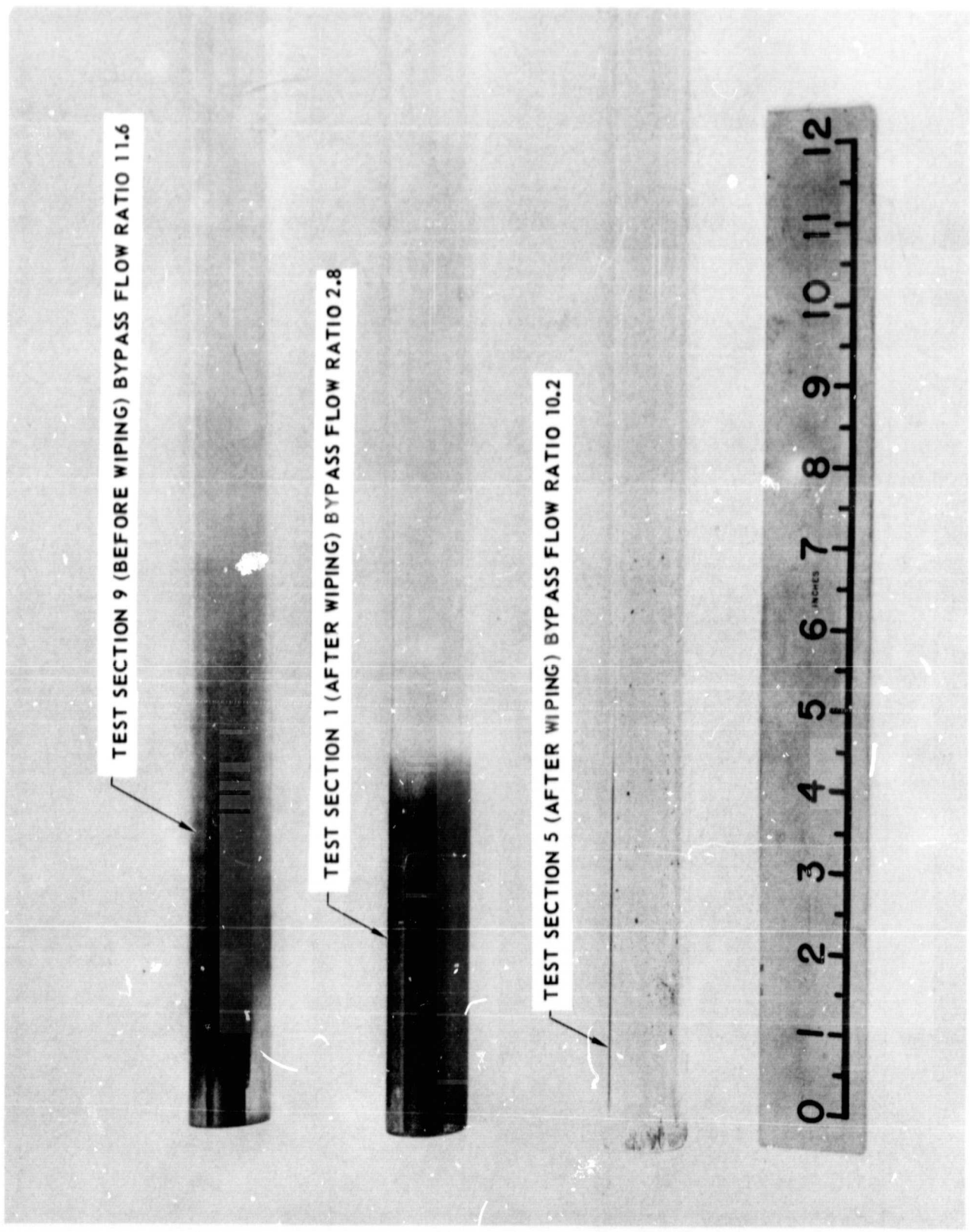

FIG. 16

PHOTOMICROGRAPHS OF ZINC PARTICLES WHICH REMAIN ON TEST SECTION WALLS AFTER TEST

TEST NO. 1, MAGNIFICATION 40,000X

BYPASS FLOW RATIO, W_B/W_T = 2.97

ZINC PARTIAL PRESSURE : BEFORE BYPASS FLOW ADDED = 0.000435 ATM

AFTER BYPASS FLOW ADDED = 0.000088 ATM

SEE TABLE III FOR ADDITIONAL TEST CONDITIONS

(a) INLET END

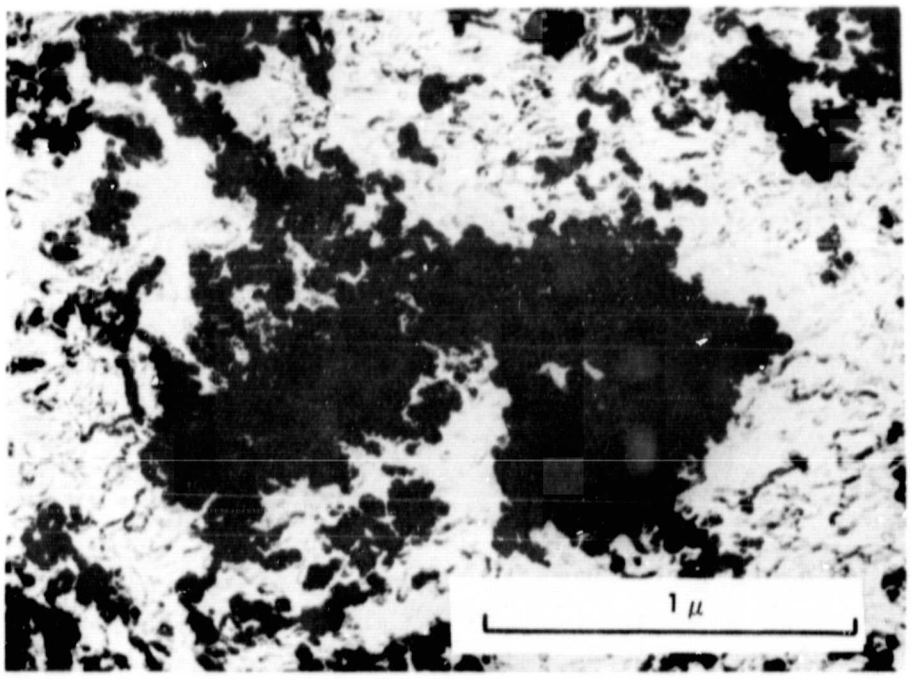

(b) OUTLET END

FIG. 17

PHOTOMICROGRAPHS OF ZINC PARTICLES WHICH REMAIN ON TEST SECTION WALLS AFTER TEST

TEST NO. 2, MAGNIFICATION 40,000X

BYPASS FLOW RATIO, $W_B/W_T = 3.4$

ZINC PARTIAL PRESSURE : BEFORE BYPASS FLOW ADDED = 0.000645 ATM
AFTER BYPASS FLOW ADDED = 0.000123 ATM

SEE TABLE III FOR ADDITIONAL TEST CONDITIONS

(a) INLET END

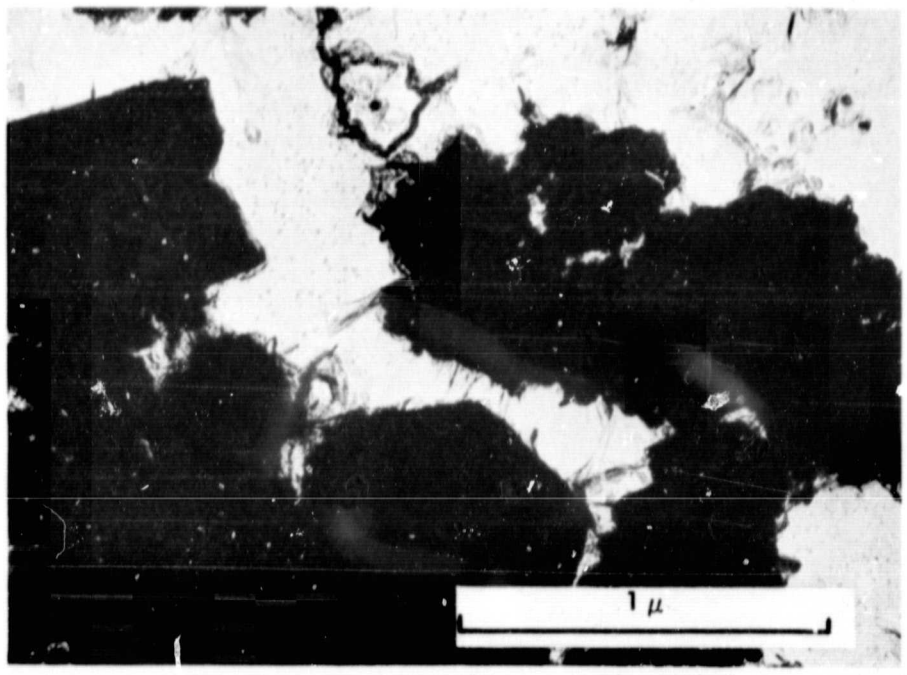

(b) OUTLET END

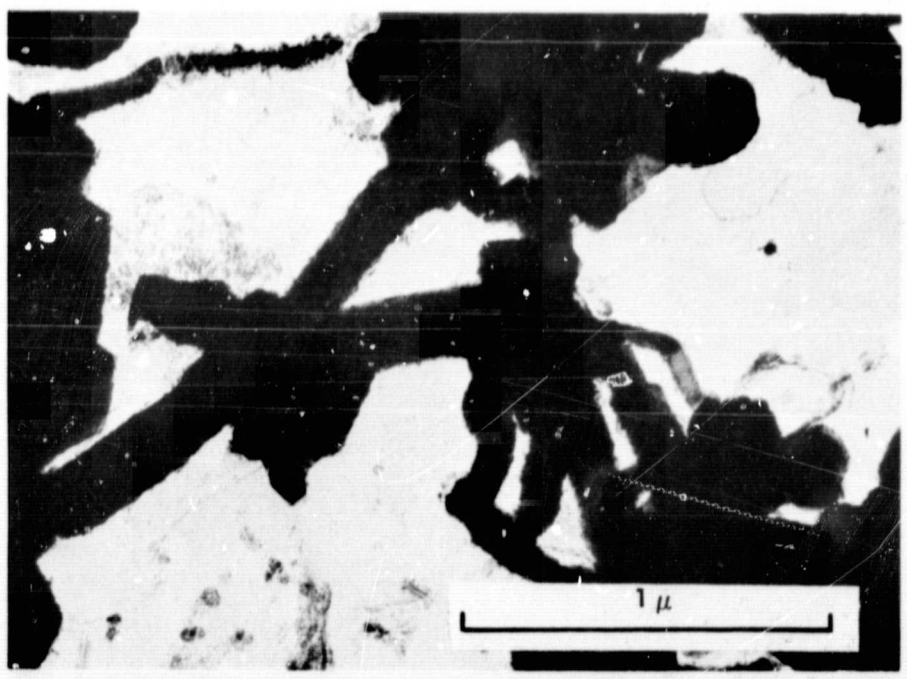

K-910900-9

FIG. 18

PHOTOMICROGRAPHS OF ZINC PARTICLES WHICH REMAIN ON TEST SECTION WALLS AFTER TEST

TEST NO. 3, MAGNIFICATION 40,000X

BYPASS FLOW RATIO, $W_B/W_T = 6.16$

ZINC PARTIAL PRESSURE : BEFORE BYPASS FLOW ADDED = 0.00153 ATM
AFTER BYPASS FLOW ADDED = 0.000185 ATM

SEE TABLE III FOR ADDITIONAL TEST CONDITIONS

(a) INLET END

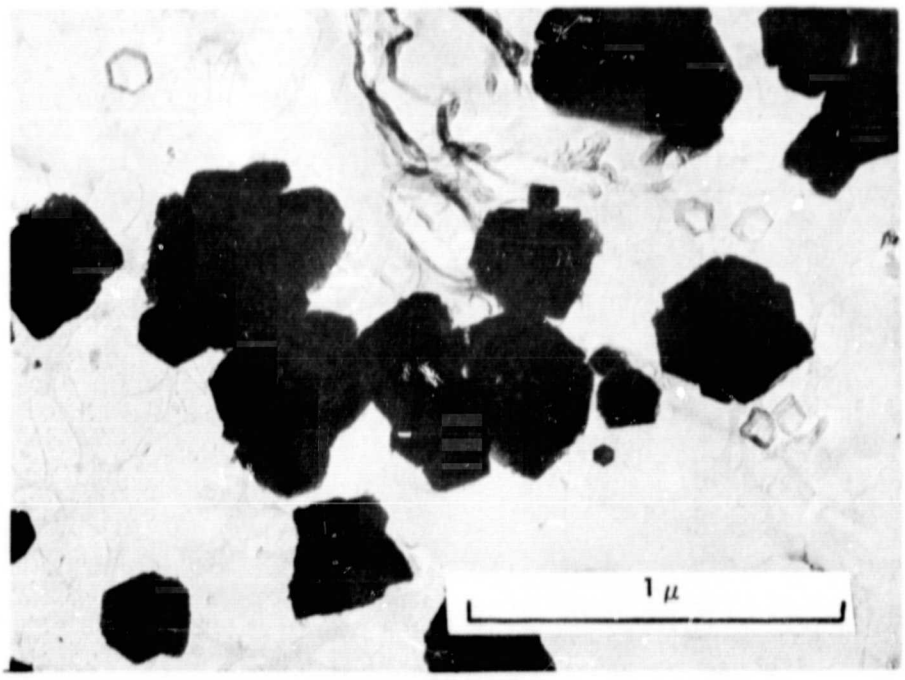

(b) OUTLET END

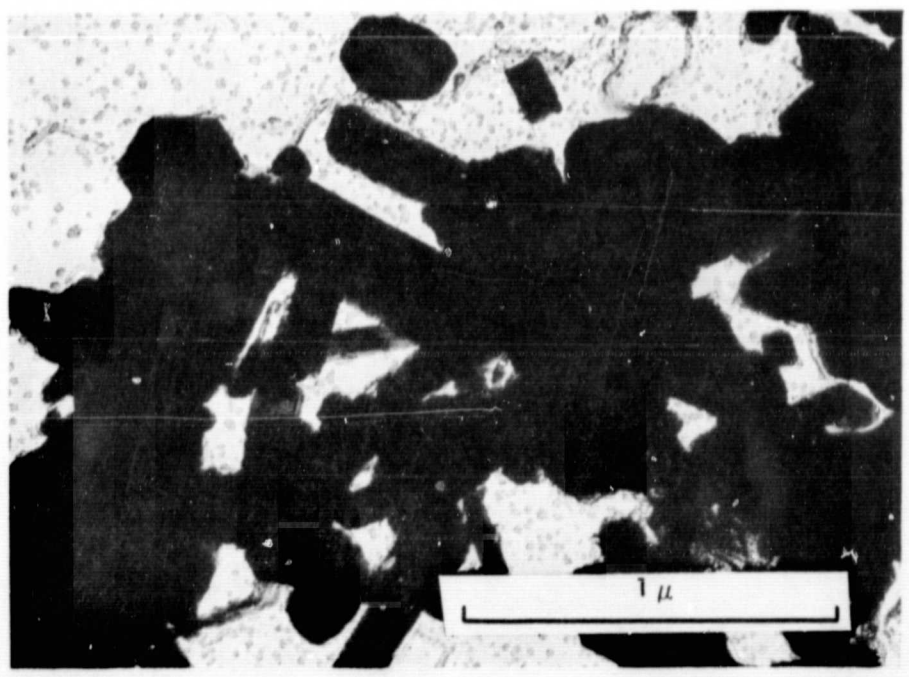

K-910900-9

FIG. 19

PHOTOMICROGRAPHS OF ZINC PARTICLES WHICH REMAIN ON TEST SECTION WALLS AFTER TEST

TEST NO. 5, MAGNIFICATION 40,000X

BYPASS FLOW RATIO, W_B / W_T = 10.2

ZINC PARTIAL PRESSURE : BEFORE BYPASS FLOW ADDED = 0.0040 ATM
AFTER BYPASS FLOW ADDED = 0.000304 ATM

SEE TABLE III FOR ADDITIONAL TEST CONDITIONS

(a) INLET END

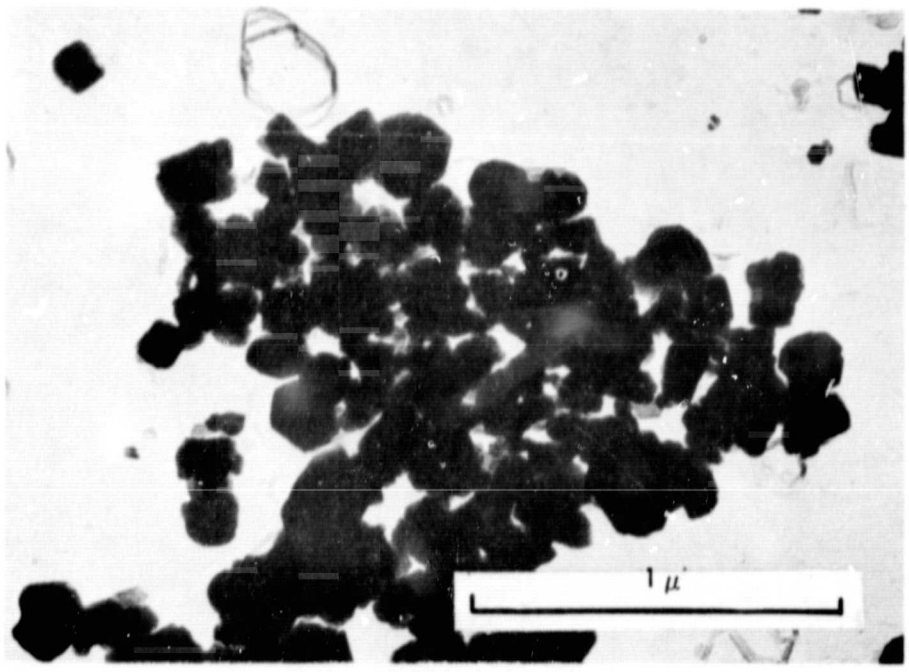

(b) OUTLET END

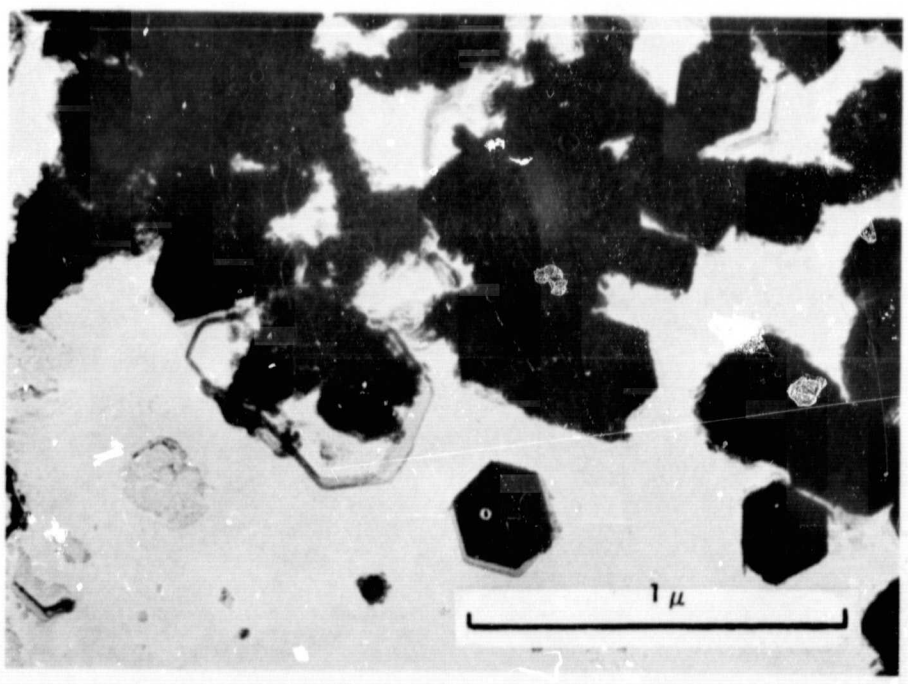

K-910900-9

FIG. 20

PHOTOMICROGRAPHS OF ZINC PARTICLES WHICH REMAIN ON TEST SECTION WALLS AFTER TEST

TEST NO. 4, MAGNIFICATION 40,000X

BYPASS FLOW RATIO, W_B/W_T = 11.05

ZINC PARTIAL PRESSURE : BEFORE BYPASS FLOW ADDED = 0.00131 ATM

AFTER BYPASS FLOW ADDED = 0.0000916 ATM

SEE TABLE III FOR ADDITIONAL TEST CONDITIONS

(a) INLET END

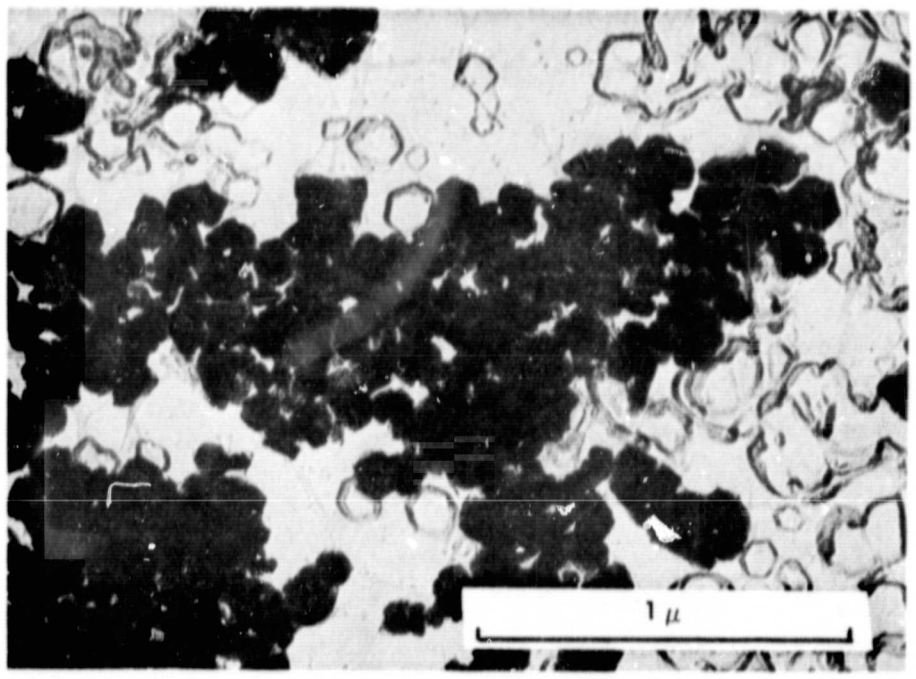

(b) OUTLET END

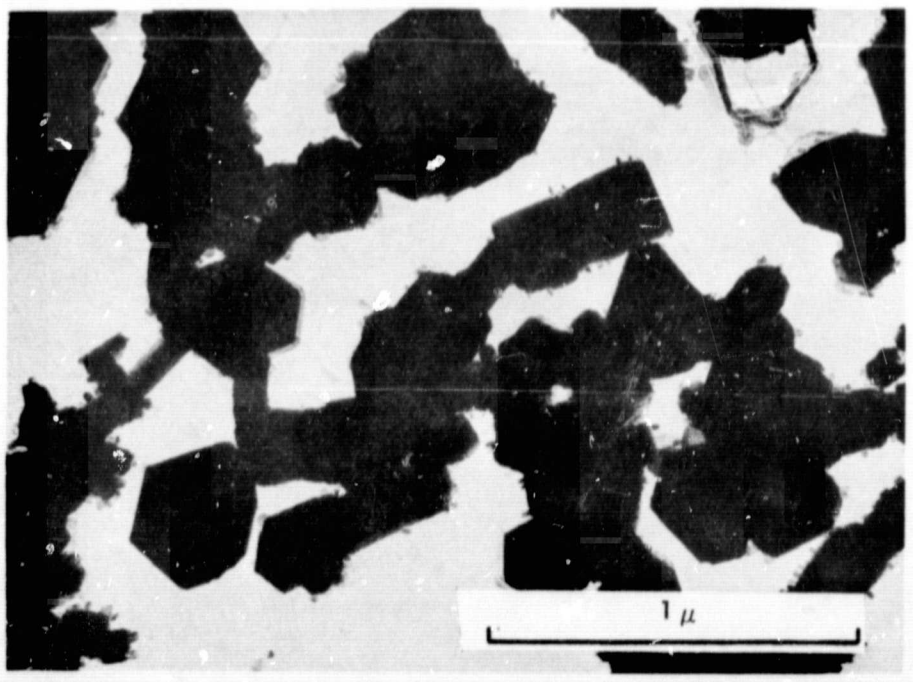

FIG. 21

POSSIBLE TEST DUCT CONFIGURATION FOR FUTURE TESTS

(a) OFF-CENTER FUEL INJECTION

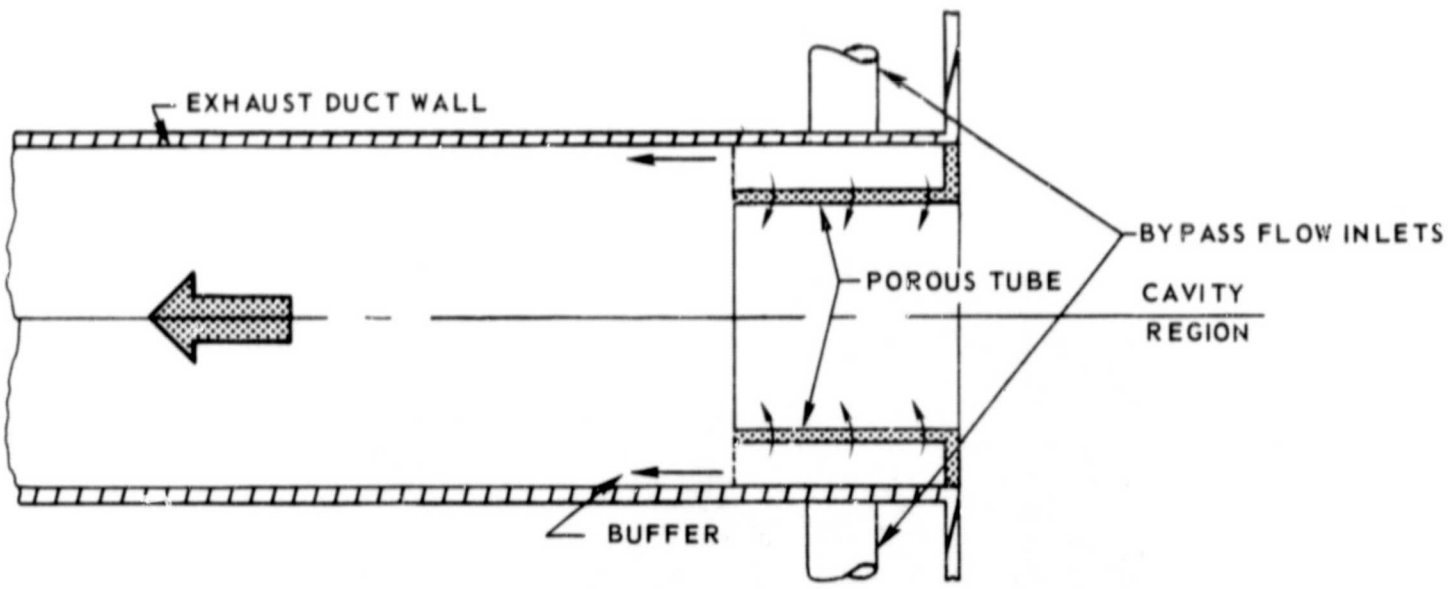

(b) CENTERLINE FUEL INJECTION